CT for Treatment Selection in Acute Ischemic Stroke: A Code Stroke Primer

Christopher A. Potter, MD
Achala S. Vagal, MD
Mayank Goyal, MD, FRCPC
Diego B. Nunez, MD, MPH
Thabele M. Leslie-Mazwi, MD
Michael H. Lev, MD

Abbreviations: ACA = anterior cerebral artery, ASPECTS = Alberta Stroke Program Early CT Score, CBV = cerebral blood volume, DWI = diffusion-weighted imaging, EVT = endovascular thrombectomy, GWD = gray-white matter differentiation, ICA = internal carotid artery, ICH = intracranial hemorrhage, LVO = large-vessel occlusion, MCA = middle cerebral artery, MIP = maximum intensity projection, tPA = tissue plasminogen activator

RadioGraphics 2019; 39:1717–1738

https://doi.org/10.1148/rg.2019190142

Content Codes: CT ER NR VA

From the Department of Radiology, Brigham and Women's Hospital, 75 Francis St, Boston, MA 02115 (C.A.P., D.B.N.); Department of Radiology, University of Cincinnati, Cincinnati, Ohio (A.S.V.); Department of Diagnostic Imaging, University of Calgary, Calgary, AB, Canada (M.G.); and Department of Radiology, Massachusetts General Hospital, Boston, Mass (T.M.L.M., M.H.L.). Presented as an education exhibit at the 2018 RSNA Annual Meeting. Received February 28, 2019; revision requested June 13 and received July 12; accepted July 25. For this journal-based SA-CME activity, the authors A.S.V., M.G., and M.H.L. have provided disclosures (see end of article); all other authors, the editor, and the reviewers have disclosed no relevant relationships. **Address correspondence to** C.A.P. (e-mail: *cpotter3@bwh.harvard.edu*).

SA-CME LEARNING OBJECTIVES

After completing this journal-based SA-CME activity, participants will be able to:

- Describe CT findings that are early indicators of ischemia and infarction.
- Compare stroke imaging patterns that are favorable or unfavorable for treatment.
- Recognize pitfalls in interpretation of nonenhanced CT images.

See rsna.org/learning-center-rg.

CT is the primary imaging modality used for selecting appropriate treatment in patients with acute stroke. Awareness of the typical findings, pearls, and pitfalls of CT image interpretation is therefore critical for radiologists, stroke neurologists, and emergency department providers to make accurate and timely decisions regarding both *(a)* immediate treatment with intravenous tissue plasminogen activator up to 4.5 hours after a stroke at primary stroke centers and *(b)* transfer of patients with large-vessel occlusion (LVO) at CT angiography to comprehensive stroke centers for endovascular thrombectomy (EVT) up to 24 hours after a stroke. Since the DAWN and DEFUSE 3 trials demonstrated the efficacy of EVT up to 24 hours after last seen well, CT angiography has become the operational standard for rapid accurate identification of intracranial LVO. A systematic approach to CT angiographic image interpretation is necessary and useful for rapid triage, and understanding common stroke syndromes can help speed vessel evaluation. Moreover, when diffusion-weighted MRI is unavailable, multiphase CT angiography of collateral vessels and source-image assessment or perfusion CT can be used to help estimate core infarct volume. Both have the potential to allow distinction of patients likely to benefit from EVT from those unlikely to benefit. This article reviews CT-based workup of ischemic stroke for making tPA and EVT treatment decisions and focuses on practical skills, interpretation challenges, mimics, and pitfalls.

Introduction

CT is the first-line imaging modality used in neurologic emergencies owing to its speed, accurate depiction of acute intracranial disease, and availability (1). The critical role of nonenhanced CT for stroke evaluation began in 1996, when the U.S. Food and Drug Administration (FDA) approved intravenous tissue plasminogen activator (tPA) for clot thrombolysis (2). Nonenhanced CT should be performed rapidly in patients with signs and symptoms of acute stroke to exclude intracranial hemorrhage (ICH) and identify large (ie, >100 mL or more than one-third of a brain territory at risk) well-established infarcts. However, the revised 2018 American Heart Association (AHA) guidelines state that the extent or severity of the hypoattenuation seen at CT should not be used as a criterion for withholding tPA owing to insufficient evidence (3). Early signs of proximal middle cerebral artery (MCA) large-vessel occlusive infarction seen at nonenhanced CT include loss of gray-white matter differentiation (GWD) at the insula, basal ganglia, and caudate head as well as sulcal effacement (4–7).

TEACHING POINTS

- Since the DAWN (Clinical Mismatch in the Triage of Wake Up and Late Presenting Strokes Undergoing Neurointervention with Trevo) and DEFUSE 3 (Endovascular Therapy Following Imaging Evaluation for Ischemic Stroke) trials showed the efficacy of endovascular thrombectomy (EVT) up to 24 hours after the onset of stroke, CT angiography has become the operational standard for rapid accurate identification of intracranial large-vessel occlusion (LVO).
- To expedite the decision to transfer a patient to a stroke center that is capable of performing EVT, all patients should undergo CT angiography immediately after undergoing nonenhanced CT without being removed from the CT scanner.
- The insula, caudate heads, and basal ganglia show early findings of proximal MCA thrombosis at nonenhanced CT and should be carefully evaluated.
- Knowledge of common stroke syndromes is part of an efficient evaluation in conjunction with interpreting CT angiograms and identifying vessel occlusions.
- Potential acute stroke mimics include intracranial masses due to primary or metastatic malignancy, cerebritis, cerebral abscess, and posterior reversible encephalopathy syndrome (PRES).

Since the DAWN (Clinical Mismatch in the Triage of Wake Up and Late Presenting Strokes Undergoing Neurointervention with Trevo) (8) and DEFUSE 3 (Endovascular Therapy Following Imaging Evaluation for Ischemic Stroke) (9) trials showed the efficacy of endovascular thrombectomy (EVT) up to 24 hours after the onset of stroke, CT angiography has become the operational standard for rapid accurate identification of intracranial large-vessel occlusion (LVO). The proximal intracranial vessels are evaluated to identify LVOs suitable for catheter thrombectomy, whereas the cervical vessels are evaluated for the presence of dissection, critical stenoses, or other vascular variants or abnormalities that may complicate EVT.

At primary stroke centers, nonenhanced CT is essential in the decision-making process by helping rule out ICH and large well-established infarct. CT angiography helps identify proximal LVOs in patients with acute MCA or intracranial internal carotid artery (ICA) syndromes, aiding in the decision of whether to transfer a patient to a comprehensive stroke center accredited to perform EVT.

However, some measure of core infarct volume is required before proceeding with EVT to determine both ICH risk and the likelihood of treatment benefit (5). Small cores (<50–70 mL or in a symmetric collateral pattern) are considered favorable for EVT treatment, and large cores (>100 mL or in a collateral pattern typical of malignancy) are considered unfavorable to treat. Core volume can be estimated from cross-sectional images (ie, diffusion-weighted images, CT angiography source images as [length × width × height]/2) (10).

Diffusion-weighted imaging (DWI) remains the unequivocal reference standard used to assess core infarct volume (3,11). When MRI is unavailable, multimodal CT assessment is helpful. Perfusion CT or multiphase CT angiography collateral and source image assessment are emerging as important tools for treating stroke in eligible patients, especially those with delayed presentation (>6 hours from symptom onset) or stroke of unknown onset (from time last seen well) (3).

This review focuses exclusively on the current role of CT in management of acute stroke. We present an overview of CT-based workup in evaluation of acute ischemic stroke that emphasizes practical considerations in nonenhanced CT, CT angiography, and perfusion CT, including key aspects of interpretation, pitfalls, and challenges.

Imaging Rationale and Code Stroke Workflow

Although an in-depth discussion of the pathophysiology of acute ischemic stroke is beyond the scope of this review, the concepts of ischemic core and penumbra are essential to understanding the role of the different components of imaging evaluation. In ischemic stroke, arterial occlusion due to embolism or less commonly in situ thrombosis leads to a cascade of cellular events. These events cause local dysfunction and ultimately cell death, leading to development of an infarct core, which is defined as brain tissue likely to die despite immediate reperfusion. The infarct core is surrounded by the ischemic penumbra, the ischemic tissue at risk for infarction that may be salvaged with timely reperfusion (12,13). In the setting of a proximal MCA or ICA LVO, if there is persistent insufficient tissue reperfusion as time passes, there is continued core infarct growth with penumbral loss (12).

The rate of penumbral loss in untreated stroke does not appear to be directly time dependent but appears to depend primarily on the quality and maintenance of collateral flow (9,10). Regardless of whether stroke patients are classified as rapid or slow progressors, failure of collateral flow with associated penumbral loss will continue up to 24 or even 48 hours after stroke onset in the absence of LVO recanalization, necessitating imaging approaches for selecting patients that may benefit from EVT (13). Accurate identification of the infarct core has therefore been a target of intense scientific investigation.

In determining a patient's eligibility for treatment of acute stroke, imaging must rapidly answer the following three essential questions: *(a)* Is there an ICH seen at nonenhanced CT that is a

contraindication to intravenous tPA or EVT, or is there a large well-established hypoattenuating infarct? *(b)* Is there a proximal LVO seen at CT angiography that can be treated with EVT? *(c)* Is there a large core infarct seen at DWI, at CT angiography of collateral vessels or on CT angiographic source images, or at perfusion CT that is a relative contraindication to intravenous tPA or EVT?

Rapidly acquiring and interpreting nonenhanced CT images of a patient suspected of having acute stroke is critical to expedite administration of intravenous tPA. Optimally, evaluation of the nonenhanced CT images of a patient designated with "code stroke" occurs at the scanner console at the time of acquisition and findings are directly communicated to the stroke team.

To expedite the decision to transfer a patient to a stroke center that is capable of performing EVT, all patients should undergo CT angiography immediately after undergoing nonenhanced CT without being removed from the CT scanner.

Performing CT angiography in this setting should never delay the administration of intravenous tPA. If a pharmacist is present as part of the code stroke team, imaging and medication preparation may occur simultaneously. Once the nonenhanced CT images have been reviewed and the decision has been made to administer tPA, CT angiography may be performed during the several minutes needed to mix and prepare the tPA.

Efficient imaging workflow is essential. Ideally, a code stroke page should be initiated as soon as the patient is identified, which may be during transportation or at presentation to the emergency department. The page notifies the stroke team, radiologists, and CT and MRI technologists about an incoming patient. This allows the technologists to accommodate the patient as quickly as possible in the scanner, minimizing the door-to-imaging time to no more than the 25 minutes recommended by the American Heart Association's Get With The Guidelines program (3,14), which can be seen at *https://www.heart.org/en/professional/quality-improvement/get-with-the-guidelines/get-with-the-guidelines-stroke/get-with-the-guidelines-stroke-overview.*

Nonenhanced CT

Technique

There has been rapid development of CT technology over the past decades, enabling rapid imaging with a relatively low dose of radiation. Current American College of Radiology recommendations for CT of the brain include a reconstructed axial section thickness of no more than 5 mm using overlapping or contiguous sections. Imaging times should be no greater than 2 seconds, with a minimum acquired section thickness of 2 mm or less and a table pitch no greater than 2:1 (15). Reformatting coronal and sagittal images is routine at many institutions, although not universal.

Dual-energy CT is available with different system architectures, the most popular being dual-source and fast kilovolt peak–switching systems. Because dual-energy CT acquires data using high and low x-ray energy spectra, materials can be characterized on the basis of their x-ray absorption characteristics and contrast can be optimized. Using the data from the low and high kilovolt peak x-ray spectra, dual-energy CT postprocessing can generate virtual monochromatic images that display the expected attenuation at a single virtual x-ray spectrum, which is not possible in conventional nonenhanced CT using a single polychromatic spectrum. Spectral absorption curves can be plotted at different energy levels and can be used to optimize the contrast of GWD on images (16,17).

Image Review

Initial Image Review.—During the initial imaging evaluation in a patient with stroke, it must be determined rapidly whether there is ICH or a large, well-established, hypoattenuating territorial infarct.

Revised 2018 American Heart Association guidelines recommend that at least 50% of stroke treatment candidates undergo nonenhanced CT imaging within 25 minutes of arrival (3). Initial rapid nonenhanced CT evaluation within 4.5 hours from onset in patients without other contraindications to intravenous tPA administration should focus on identification of a large territorial infarct and exclusion of ICH, which is an absolute contraindication to intravenous tPA treatment (3).

These results should be communicated immediately after imaging to enable rapid intravenous tPA administration, which should never be delayed by CT angiography for EVT triage. Currently, guidelines for treatment with intravenous tPA within 4.5 hours and EVT within 6 hours are based only on nonenhanced CT relative and absolute exclusion criteria (3,14).

The sensitivity and specificity of nonenhanced CT for depiction of ICH is estimated to be high with modern CT scanners, likely exceeding 95%–98% depending on the patient cohort and level of training of the radiologists (18). Indeed, recent work published in *Nature Biomedical Engineering* has suggested that even subtle hemorrhages can be sensitively depicted with artificial intelligence platforms, with accuracy approaching that of experienced subspecialty-trained neuroradiologists and exceeding that of less experienced non–subspecialty-trained readers (19).

Nonenhanced CT is much less sensitive compared with DWI for depiction of both the cytotoxic edema and low cerebral blood volume (CBV) that accompany early ischemia (13). Despite this, the widespread availability and speed of CT make it the most practical first-line imaging strategy at most institutions, as it can be performed in minutes and requires no prescreening or patient exclusion.

The sensitivity and specificity for acute infarction at nonenhanced CT likely depend on the duration, infarct size, and degree of ischemia. Sensitivity and specificity for depiction of early ischemic change are also likely better for the anterior circulation than the posterior circulation, primarily owing to artifact at the skull base from thick surrounding bone, although this has not been definitively demonstrated.

Several areas of the brain including the insula, basal ganglia, and caudate head are early indicators of acute infarct owing to their vascular anatomy in relation to the most common patterns of proximal MCA LVO distribution (4,5,20). Special attention should therefore be directed to these regions during initial image review (Fig 1).

Well-established frank ischemia seen at CT in these regions as an area of low attenuation with loss of GWD is typically attributed to vasogenic edema from blood-brain barrier breakdown. This imaging finding indicates irreversible infarction in the clinical setting of an acute MCA occlusion and is not attributable to cytotoxic edema from membrane pump failure and low CBV with poor collateral flow (21). Cytotoxic edema is a more subtle hyperacute finding and is typically attributable to membrane pump failure and low CBV.

The Alberta Stroke Program Early CT Score (ASPECTS) was developed to establish a reproducible scoring system for early ischemic changes at nonenhanced CT due to MCA stroke, since estimation of one-third of the MCA territory can be challenging in practice (22).

In the ASPECTS system, the brain is separated into 10 discrete labeled areas of the deep and superficial gray matter on each side. Starting with a maximum of 10 points on each side, the patient's score is decreased by one point for each area of the brain with early ischemic change (Fig 2). As it is a topographic scoring strategy, it requires only axial images for implementation.

The nonenhanced CT ASPECTS is often used by stroke neurologists to identify the extent of early ischemic change. Patients with ASPECTS of less than 7 have been shown to have a lower chance of independent recovery after a stroke (22). Automated quantification of ASPECTS using machine learning is being implemented at some sites (23). More information about ASPECTS can be found at the educational website *www.aspectsinstroke.com*.

Identification of vessel occlusion is limited at nonenhanced CT, although an "attenuating vessel sign" is highly specific when it is present. The attenuating vessel sign due to thrombus in the M1 segment of the MCA has relatively low sensitivity of 17%–52% but high specificity of 95% (24,25).

Considered an equivalent of the attenuating vessel sign in the M1 segment, the MCA "dot" sign in the proximal M2 vessels is often associated with early insular GWD loss (26). At imaging, the dot sign appears in the vessels in the lateral sylvian fissure adjacent to the insula wall.

The mixed images obtained with dual-energy CT are produced by blending both high and low kilovolt peak datasets. Dual-energy CT can be used in the initial examination similar to the way conventional nonenhanced CT is used. Monochromatic imaging is not widely used in this context, since image reconstruction is not typically automated and it is too time-consuming. Nevertheless, optimization of GWD has been reported to occur at a virtual kilo–electron voltage of 66–75 (17).

Tip or Pearl for Image Review.—A methodical search pattern is important because the imaging findings in acute ischemic stroke can be subtle on nonenhanced CT images.

Gray-White Matter Differentiation.—Loss of GWD is the imaging hallmark of acute infarct at nonenhanced CT. Use of a narrow stroke window while performing soft-tissue sequences has been studied, and recommended values have been reported (window width, 8 HU; window level, 32 HU) (27).

Evaluation of coronal and sagittal images is essential because signs of sulcal hemorrhage on axial images are subtle and can easily be missed. The imaging findings of acute infarct can be difficult to notice in the following locations: the extreme vertex owing to volume averaging; the inferior temporal lobes, where the gray-white matter junction is oriented axially; the occipital lobes owing to frequent artifact caused by the irregular contours of the skull; and the deep gray matter, particularly the caudate heads (Fig 3) (4). The insula, caudate heads, and basal ganglia show early findings of proximal MCA thrombosis at nonenhanced CT and should be carefully evaluated.

However, nonenhanced CT has low sensitivity for depiction of hyperacute and early acute hypoattenuating ischemic changes (28). Even large territorial infarcts may not be seen until the subacute phase. An acute territorial infarct visible at nonenhanced CT that is greater than one-

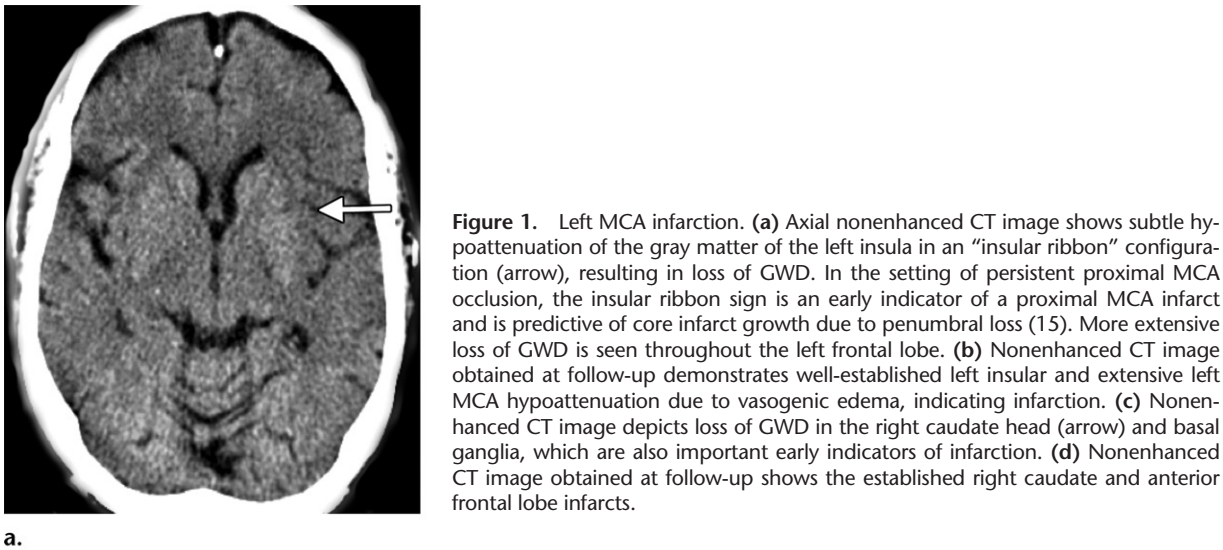

Figure 1. Left MCA infarction. **(a)** Axial nonenhanced CT image shows subtle hypoattenuation of the gray matter of the left insula in an "insular ribbon" configuration (arrow), resulting in loss of GWD. In the setting of persistent proximal MCA occlusion, the insular ribbon sign is an early indicator of a proximal MCA infarct and is predictive of core infarct growth due to penumbral loss (15). More extensive loss of GWD is seen throughout the left frontal lobe. **(b)** Nonenhanced CT image obtained at follow-up demonstrates well-established left insular and extensive left MCA hypoattenuation due to vasogenic edema, indicating infarction. **(c)** Nonenhanced CT image depicts loss of GWD in the right caudate head (arrow) and basal ganglia, which are also important early indicators of infarction. **(d)** Nonenhanced CT image obtained at follow-up shows the established right caudate and anterior frontal lobe infarcts.

a. b. c. d.

third of the MCA territory has been considered a relative contraindication for administration of intravenous tPA, but the revised 2018 American Heart Association guidelines state that the extent or severity of the hypoattenuation should not be used as a criterion for withholding intravenous tPA owing to lack of sufficient evidence (3).

Sulci.—Focal sulcal effacement is also an important early secondary sign of acute ischemia and can help identify subtle acute infarcts.

Vessels.—The hyperattenuating vessel sign can be seen in the intracranial ICA, M1 and M2 segments of the MCA, and A1 and A2 segments of the anterior cerebral artery (ACA) as well as the basilar and vertebral arteries (29) (Fig 4). This sign typically indicates the need for intervention. Although CT angiography should always be performed for definitive diagnosis in LVO, identification of a hyperattenuating MCA sign greater than 8 mm in length also indicates that administration of intravenous tPA alone is not likely to achieve successful recanalization. This is not an indication to withhold intravenous tPA according to the revised 2018 American Heart Association guidelines (3,30).

In addition to reviewing the nonenhanced CT images for acute infarct, it is important to remember that mimics of acute stroke are common in the emergent setting. A full routine evaluation of the nonenhanced CT images is essential to identify alternative diagnoses such as intracranial masses, infection, and hemorrhage, all of which can cause focal and nonspecific neurologic findings.

Pitfalls of Image Review.—Challenges in evaluation of nonenhanced CT images in stroke are often caused by artifact from patient motion that can be associated with alterations in consciousness as well as from streak artifact from bone or hardware (26). Skull base artifact at the petrous apices or posterior fossa often limits the visibility of subtle hypoattenuation in acute infarct (Fig 3). Skull base streak artifact can also mimic the

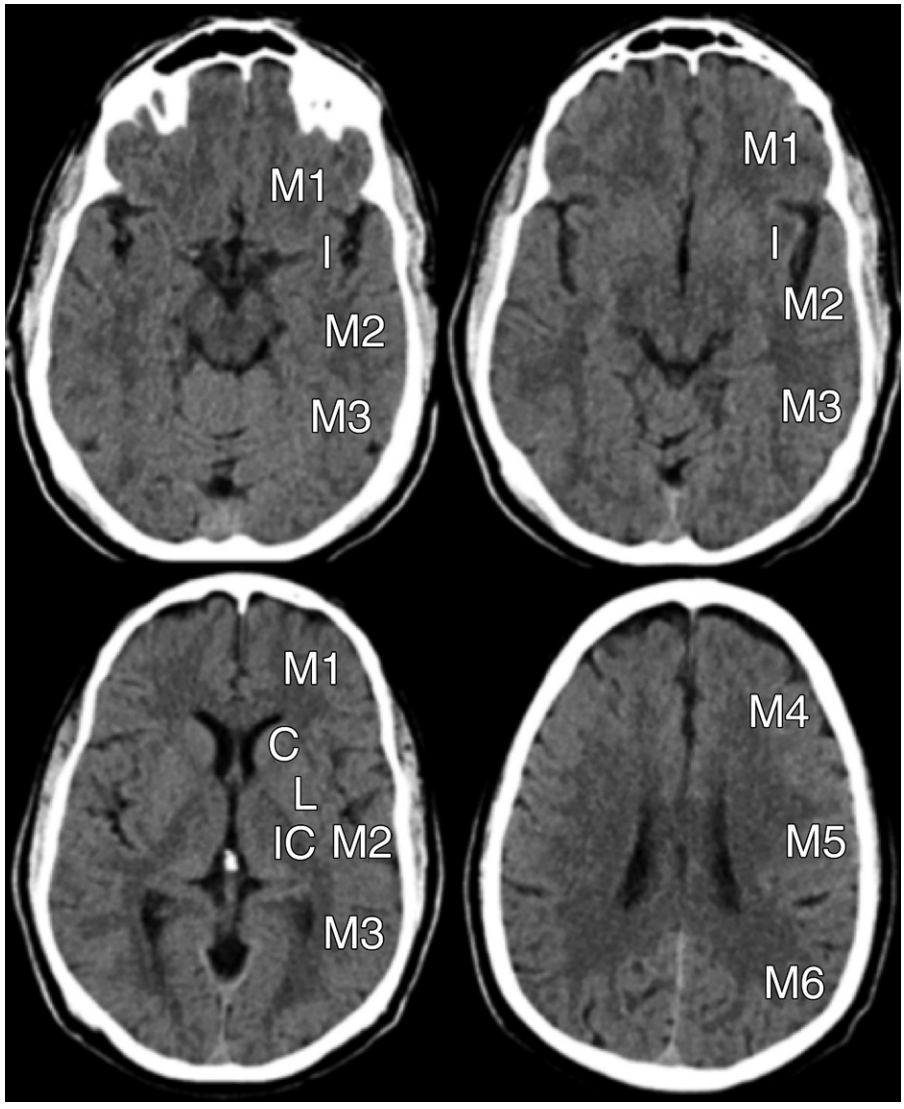

Figure 2. Regions of the brain used to calculate ASPECTS. Axial nonenhanced CT images show the labeled MCA territories that are given one point each for a score out of 10 points by using the ASPECTS system. *C* = caudate, *I* = insula, *IC* = internal capsule, *L* = lentiform nucleus, *M1–M6* = cortical regions.

hyperattenuating MCA sign. Comparison with the contralateral side will typically help resolve any ambiguity.

Coronal and sagittal reformations can improve visualization and help one distinguish artifact, infarct, and hemorrhage in some cases, especially at locations such as the sylvian fissure, where axial volume averaging can mimic GWD loss. In situations where axial images are tilted off axis, coronal and sagittal reformations can display areas of nonanatomic linear hyperattenuation that cross through different brain regions and structures.

Evaluation of the basilar artery for acute thrombus is another example where coronal and sagittal reformations can be helpful for distinguishing artifact from thrombus.

CT Angiography

Technique

Intravenous tPA administration should never be delayed to perform advanced CT, and CT angiography should also never be delayed by removing the patient from the CT table for additional clinical evaluation or to review the nonenhanced CT images at the scanner.

An 18–20-gauge needle should be confirmed before the patient arrives, as power injection of contrast material is required. The right arm should be used to limit streak artifact from hyperattenuating contrast material crossing the midline, since the flow from the left brachiocephalic vein enters the superior vena cava at an average rate of 4–5 mL/sec in adults.

Administration of iodinated contrast material without first testing renal function in candidates for EVT is acceptable, as the likelihood of contrast material–induced nephropathy has been shown to be very low relative to the potential for brain injury from stroke (3,31). Correct timing of the injection of contrast material can be achieved by using a test bolus to calculate the imaging delay or by using semiautomated or automated triggering after injection of the full dose of contrast material.

Figure 3. Potential pitfalls that can cause missed infarcts at nonenhanced CT. **(a)** Small focus of GWD loss at the right frontal vertex (arrow), which could be missed owing to atypical location just deep to the skull, especially with thick (≥5-mm) axial sections. **(b)** Left inferior cerebellar GWD loss (arrow) might also be overlooked owing to skull base beam-hardening artifact in this region. **(c)** Subsequent diffusion-weighted image shows the evolving infarct. **(d–f)** The presence of nonstroke disease can also distract the reader owing to satisfaction of search or anchoring bias, as well as nonspecific findings. **(d, e)** In another patient, low attenuation due to vasogenic edema from a left temporal meningioma (white arrow in **d**) distracts from and overlaps with hypoattenuation from an acute left anterior frontal infarct (black arrow in **d**). **(f)** Diffusion-weighted image shows the acute left anterior frontal infarct. **(g, h)** Similarly, encephalomalacia from prior infarcts makes evaluation for new infarction difficult. **(g)** In a patient with old right MCA–distribution encephalomalacia, CT image shows new left frontal GWD loss (arrow) due to an acute left MCA infarct, which might be considered "age-indeterminate." **(h)** Subsequent MR image shows the acute left MCA infarct.

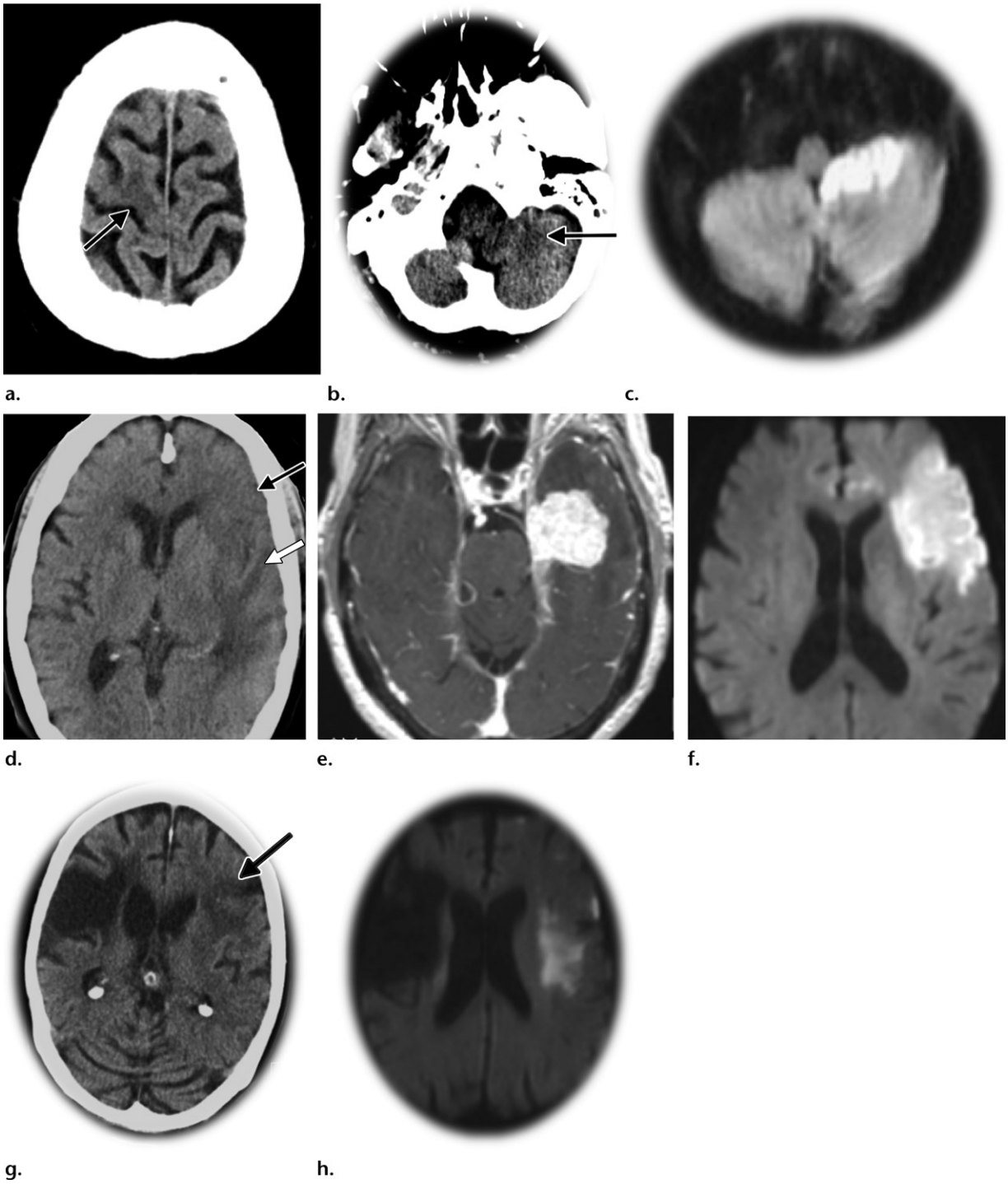

Images should be acquired at a maximum thickness of 1.5 mm and reconstructed in sections overlapping by 50% or less. Anatomic coverage should begin at the origins of the cervical vessels at the aortic arch and extend through the vertex (32). Multiplanar and maximum intensity

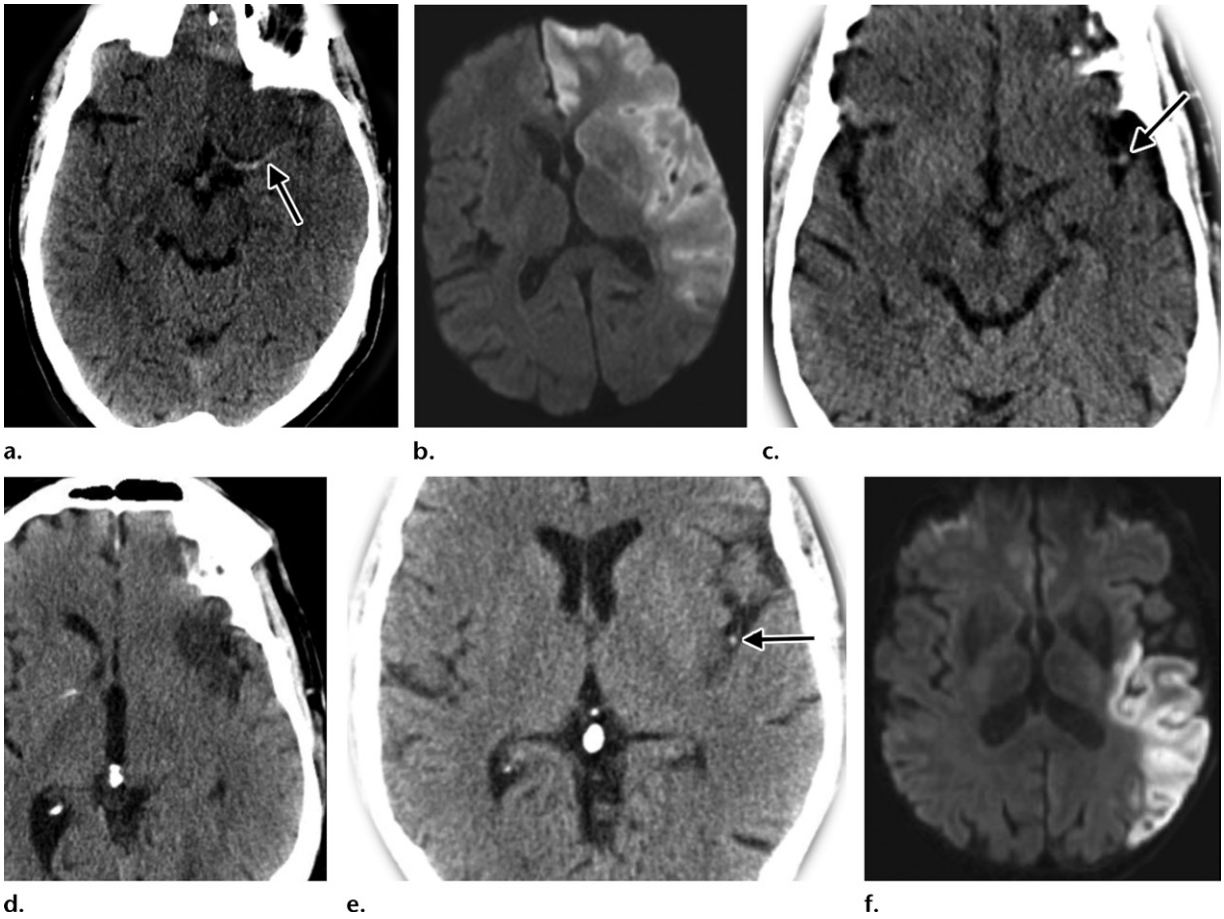

Figure 4. Attenuating vessel sign. This is an early hyperacute ischemic finding at nonenhanced CT that can be seen before changes of vasogenic edema are visible and allows anticipation of the presence of a clot at CT angiography for both anterior and posterior circulation strokes (24). **(a)** A hyperattenuating MCA sign (arrow) is seen in the M1 segment. **(b)** Diffusion-weighted image shows a large left MCA infarct. **(c)** Thrombus in an M2 branch vessel can create an MCA dot sign, seen in the left anterior sylvian fissure (arrow). **(d)** Subsequent nonenhanced CT image shows a left MCA infarct in the territory of the left anterior temporal artery. **(e)** An MCA dot sign is seen in another patient in the posterior sylvian fissure (arrow). **(f)** Follow-up diffusion-weighted image shows the extent of the infarct, which corresponds to the occlusion of the inferior MCA M2 division.

projection (MIP) reformations can be acquired at orthogonal planes for optimal evaluation, depending on the institution.

CT angiography can be performed as a single, delayed, or multiphasic study. Multiphasic CT angiography begins with an arterial imaging sequence spanning from the aortic arch to the vertex. The next two imaging sequences are performed after a single contrast material bolus and are timed to depict the peak and late venous phases in the head (33). The images acquired with multiphasic CT angiography can be rapidly and automatically reformatted into sequential axial MIP images that can be used for collateral flow assessment and EVT decision making (33).

Four-dimensional CT angiography is performed at some centers. This is a dynamic CT angiographic technique in which bone-subtracted MIP images can be viewed like digital subtraction angiograms are viewed over time. The images are used to evaluate collateral filling or in a condensed three-dimensional MIP image of all time points (Fig 5) (34). Automated delineation of LVOs is under investigation as well, which may help to speed detection, particularly in busy centers.

CT angiographic data can be acquired at dual-energy CT as well, which has the potential to provide robust three-dimensional vessel reconstruction using bone subtraction techniques (16,35,36). The lengthy postprocessing time has largely limited its clinical application. In addition, iodine maps are reconstructions that can be used to show attenuating contrast material throughout an image. The attenuation can also be subtracted from an image to create a virtual nonenhanced CT image (37).

Image Review

Tips or Pearls for Image Review.—Patients suspected of having LVO should undergo CT angiography to expedite treatment with EVT. Although the entire intracranial vasculature is depicted well at current-generation CT angiography, occlusions of the intracranial ICA and

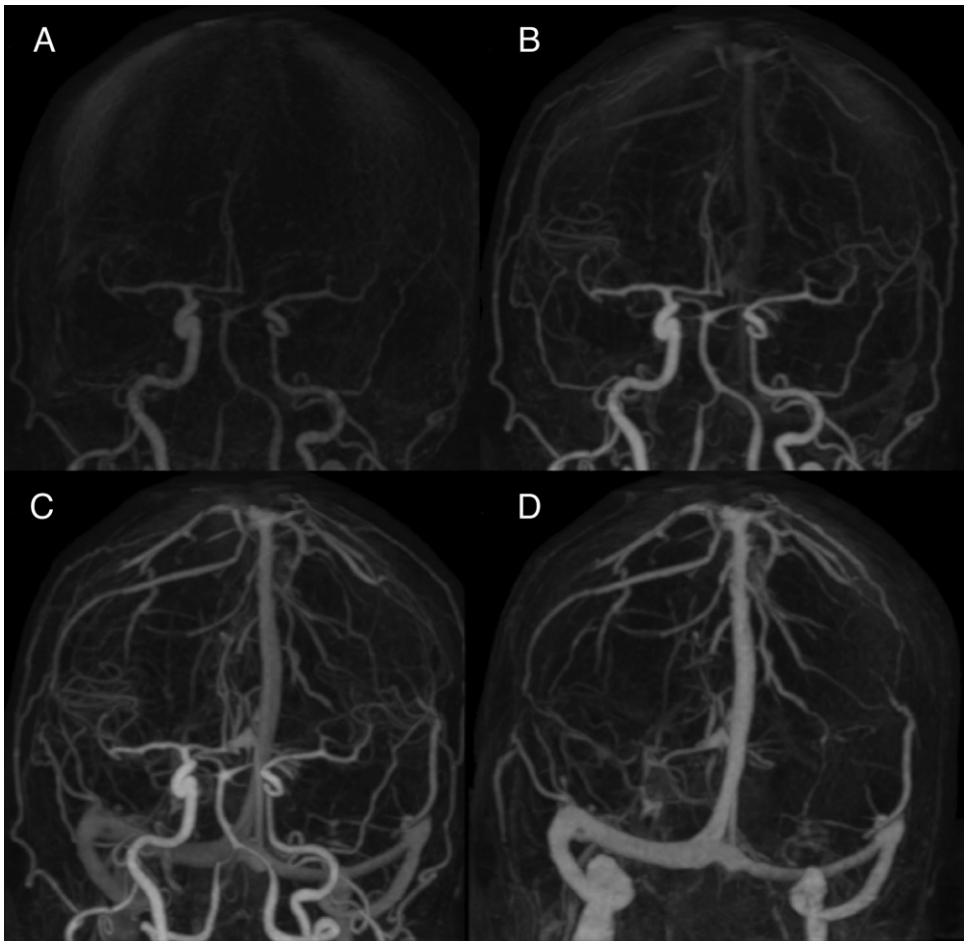

Figure 5. Four-dimensional CT angiography. Dynamic four-dimensional CT angiography data can be reconstructed into time-resolved MIP reconstructions that appear similar to conventional catheter digital subtraction angiograms. The earliest images show the arteries *(A)*, followed by increased venous filling over time (*B*, *C*) and dense opacification of the venous sinuses without visible arterial enhancement *(D)*.

proximal MCA segments should be the focus at imaging, since these vessels are the targets for EVT (3). The skull base and neck vessels are largely orthogonal to the axial imaging plane, and their patency can be assessed quickly by viewing the axial CT angiography source images at the scanner console at the time of acquisition.

Overlapping thick-section MIP images of the circle of Willis in axial, coronal, and sagittal planes can help expedite identification of LVOs (3-cm section thickness at overlapping intervals of 5 mm). The more distal branches of the circle of Willis can be difficult to interpret on thin-section CT angiography source images, and using thick-section reconstructions increases their visibility. CT technologists can produce MIP reformations at the scanner console in less than 1 minute (28,38).

Collateral flow assessment of the intracranial circulation at CT angiography can be used to help assess the potential risks (ie, ICH) versus benefits (ie, limited infarct growth and improved clinical outcomes) of EVT. The quality of collateral flow is an important determinant of the rate of infarct progression (12).

Multiple groups and studies have described systems that help define collateral flow, including ASPECTS, the Miteff and Maas systems, and the modified Tan scale (39–41). There is no consensus on which standardized scoring system is optimal for collateral grading.

Several groups consider a malignant collateral pattern at delayed phase CT to be characterized by contrast material failing to reach more than 50% of the intracranial vessels and tissue bed of the at-risk MCA territory (42). Conversely, a good collateral pattern can be defined as a symmetric or nearly symmetric leptomeningeal flow when comparing the hemisphere affected by ischemia with the contralateral hemisphere. In the setting of an intracranial ICA or proximal MCA occlusion, infarct core growth and penumbral loss progress more rapidly in patients with malignant collateral patterns (ie, fast progressors), whereas infarct core growth and penumbral loss progress more slowly in patients

with good collateral patterns (ie, slow progressors) (43,44).

ASPECTS is one of the best-known collateral score systems and compares the filling of the intracranial arteries at all three phases of multiphase CT angiography. When there are no or just a few vessels visible in the ischemic territory at any phase, the collateral score is given a 0 or 1, indicating poor collaterals. If there is normal symmetric vessel filling, or a delay of a single phase with similar extent of vessel filling, collaterals are given a score of 5 or 4, respectively, indicating good collaterals. Intermediate collaterals with scores of 2 or 3 demonstrate a delay of two phases with either a similar or decreased extent of perfused vessels (Fig 6) (45).

Modified by the time of stroke onset, the degree of collateral flow is an important indicator of the potential efficacy of EVT. Malignant or poor collateral flow is associated with a low probability of penumbral salvage or clinical benefit from EVT unless thrombectomy is performed very quickly after onset of stroke (33,46) (Fig 7).

Complete assessment of the intracranial vasculature can seem daunting. MIP and multiplanar reformations are indispensable for efficient assessment. Coronal reformations rapidly depict the proximal MCA, ACA, and terminal ICA, while sagittal reformations demonstrate the ACA and distal MCA vessels. Evaluating the overall symmetry of vessels can help identify regions of relative hypoperfusion, particularly in the cerebral convexities. Assessing hypoperfused regions can help differentiate stroke from mimics such as seizure and directs the reader's attention to likely areas of vessel occlusion.

Knowledge of common stroke syndromes is part of an efficient evaluation in conjunction with interpreting CT angiograms and identifying vessel occlusions. Although a patient's signs and symptoms may not be available at the time of their imaging orders, discussing the results of the initial nonenhanced CT with referring providers often offers the opportunity to obtain a brief clinical history that can help focus the CT angiography assessment. Knowledge of symptoms such as laterality, acuity of onset, and specific functional involvement (eg, aphasia, hemiparesis, hemisensory deficit, and hemineglect) is essential to correlate specific imaging findings with the acute manifestation of stroke.

For example, contralateral arm and face weakness with or without a sensory disturbance, which might also include an expressive aphasia (Broca aphasia) in the dominant hemisphere (typically the left hemisphere), suggests occlusion of the superior M2 division or anterior temporal MCA branches (Fig 8a). The superior M2 division is located anteriorly in the sylvian fissure and primarily supplies the superior frontal-parietal regions. A receptive aphasia (Wernicke aphasia) in the dominant hemisphere or visual field problems from disruption of the visual tracts suggest occlusion of the inferior M2 division of the MCA (Fig 8b). The inferior M2 division is in the posterior sylvian fissure and supplies the temporal-parietal regions.

A combination of these symptoms suggests occlusion more proximally at the MCA bifurcation (Fig 8c). Complete hemiplegia and hemisensory loss suggest a proximal M1 segment MCA occlusion, which includes occlusion of the lenticulostriate vessels that supply the internal capsule (Fig 8d).

Isolated focal arm, hand, and face weakness suggests a more distal occlusion, usually in an M3 or M4 branch. These occlusions are depicted well on sagittal thick-section MIP images.

Complete hemiplegia and hemisensory loss can also be caused by occlusion of the intracranial ICA. Dense monocular blindness can also occur and is due to an occlusion of the ophthalmic artery. However, occlusion of the ICA may be more difficult to detect. The symptoms can range from subtle to severe, and there may be no symptoms if the circle of Willis is intact and there is good contralateral flow (47).

Contralateral lower extremity weakness and sensory loss suggest occlusion of the ACA (Fig 8e). Occlusion of the A1 segment of the ACA is an easily overlooked cause of infarct in the anterior lentiform nuclei and caudate head.

Visual changes are the most frequent sign of posterior cerebral arterial occlusion. These changes typically manifest as homonymous hemianopsia owing to infarction of the occipital visual cortex.

Profound alteration of consciousness or cranial nerve deficits suggest brainstem involvement and basilar thrombosis. Readers should always check for the presence of these conditions, and they are usually clearly depicted at CT angiography.

Although symptoms of ataxia, vertigo, and dizziness are nonspecific, they should prompt careful evaluation of the posterior circulation, including the posterior inferior cerebellar artery (PICA) (Fig 8f) and anterior inferior cerebellar artery (AICA). The distribution of vessels supplying the cerebellum is highly variable. The AICA and PICA develop in a reciprocal relationship, and a single artery or side could be dominant. If the ipsilateral PICA and AICA are not visible at imaging, this may indicate vascular occlusion and prompts careful evaluation (47).

The degree and location of vessel narrowing or partial obstruction should be included in the final interpretation. Intracranial arterial stenosis

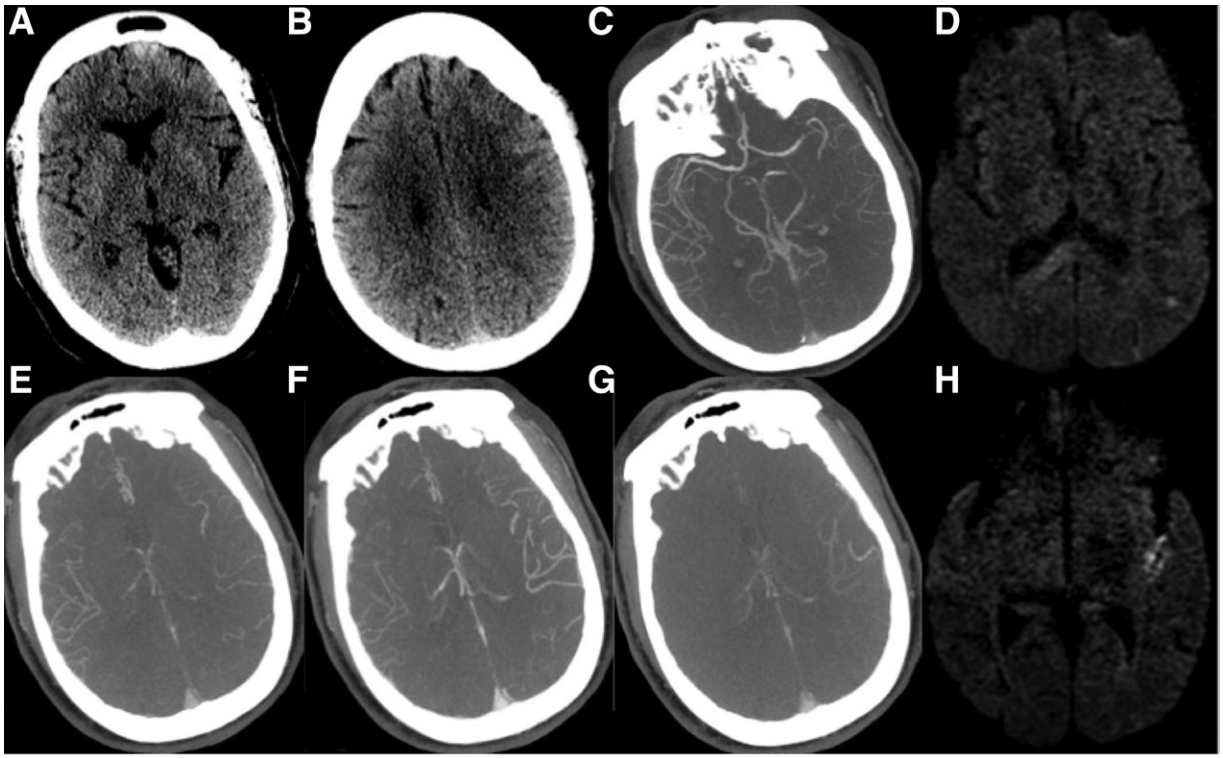

a.

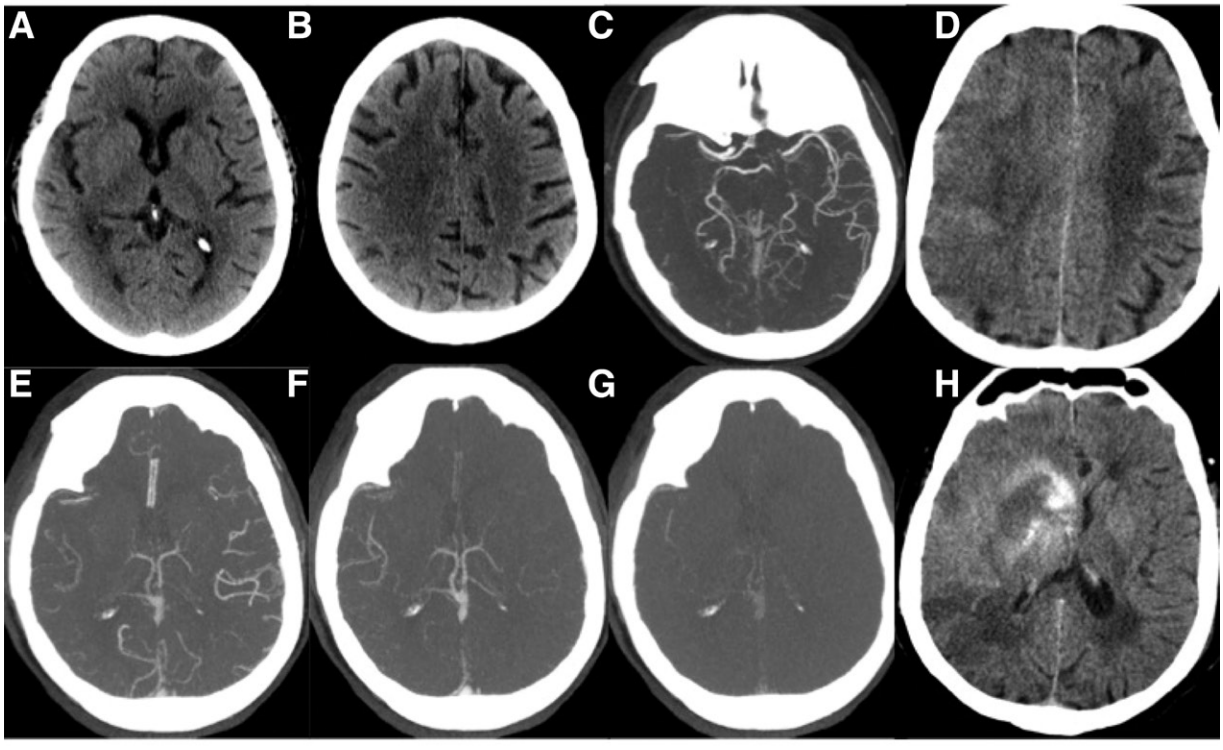

b.

Figure 6. **(a)** Good collateral flow. *A* and *B*, Initial nonenhanced CT images show some patchy GWD loss in the left anterior frontal lobe. *C*, Axial MIP CT angiogram shows occlusion at the left MCA bifurcation. *E–G*, MIP images of the three sequential CT angiography phases show that the extent of the visualized vessels on the affected side has a single phase delay, consistent with good collaterals. *D* and *H*, Diffusion-weighted images after treatment with intravenous tPa and EVT demonstrate that only a small focus of acute infarct remains. **(b)** Poor collateral flow. *A* and *B*, Initial nonenhanced CT images depict no loss of GWD. *C*, Axial MIP image from CT angiography shows occlusion of distal right M1. *E–G,* MIP images of the three sequential CT angiography phases show few opacified vessels on the affected side, consistent with poor collaterals. The patient was treated with intravenous tPA and EVT. *D* and *H,* Follow-up nonenhanced CT images show a large right MCA infarct that developed after treatment.

Figure 7. Collateral flow at multiphase CT angiography with right-sided M1 occlusion. **(a)** ColorViz software summation images—with color-coded early arterial (red), late arterial or venous (green), and delayed venous (blue) phases—show predominantly green vessels (arrowheads) ipsilateral to the right MCA occlusion (arrow), indicating symmetric but delayed collaterals relative to the predominantly red vessels in the unaffected hemisphere and suggesting good pial arterial filling collateral flow. **(b)** Corresponding conventional multiphase CT angiograms. The patient received intravenous tPA. **(c)** Follow-up diffusion-weighted images 24 hours after ictus show hyperintense signal consistent with acute infarction in the caudate head and lentiform nucleus only with sparing of the cortex, where good collateral flow was present.

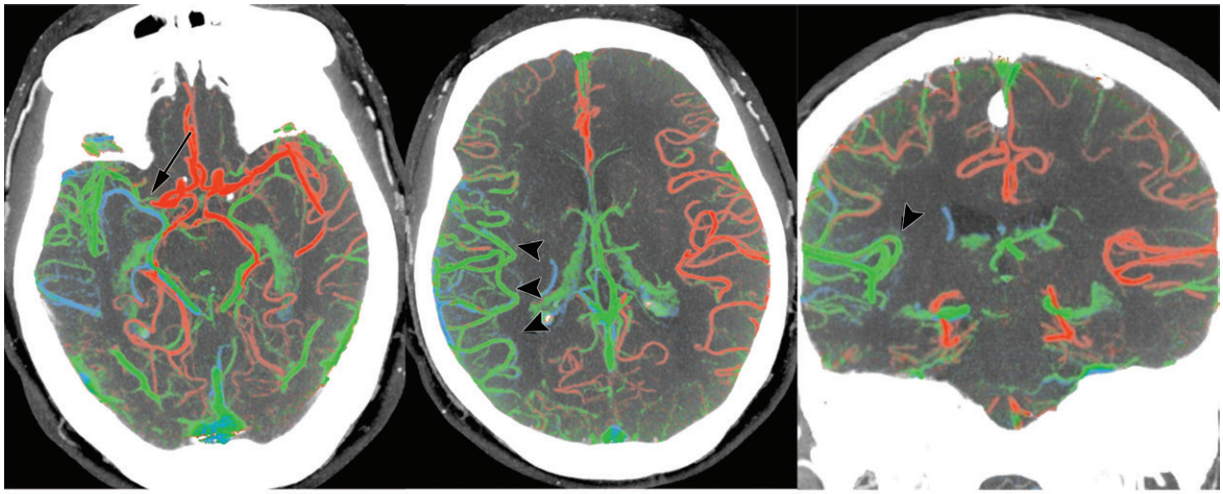

a.

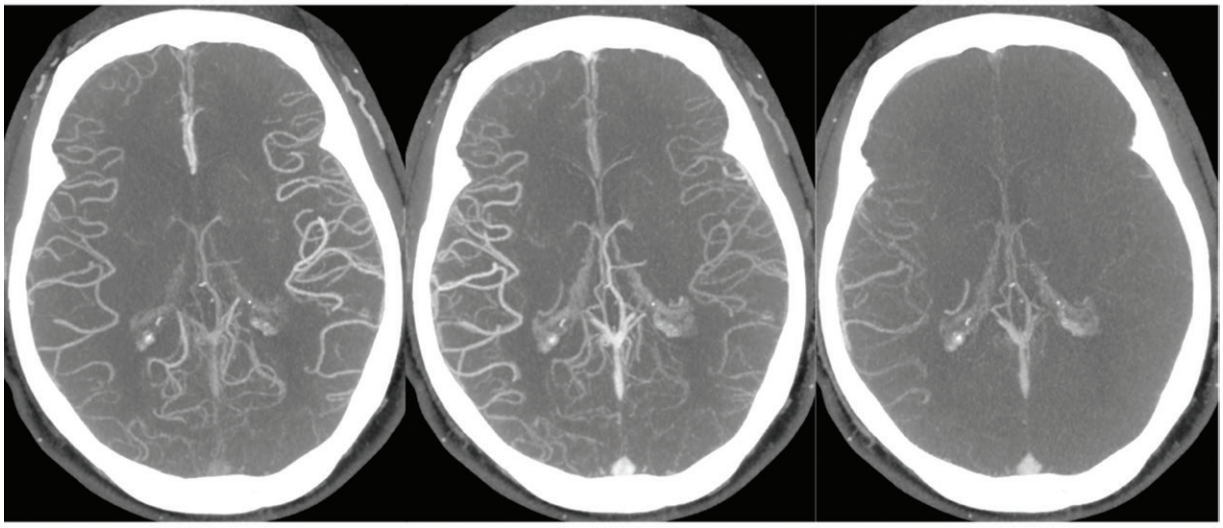

b.

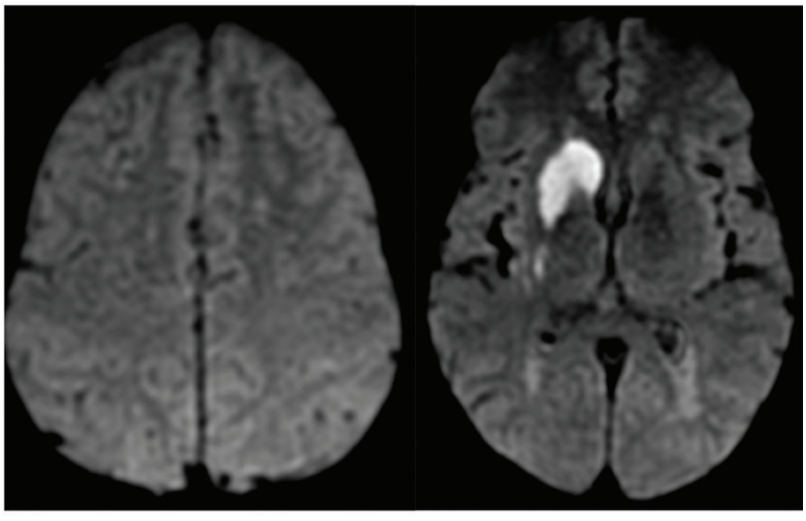

c.

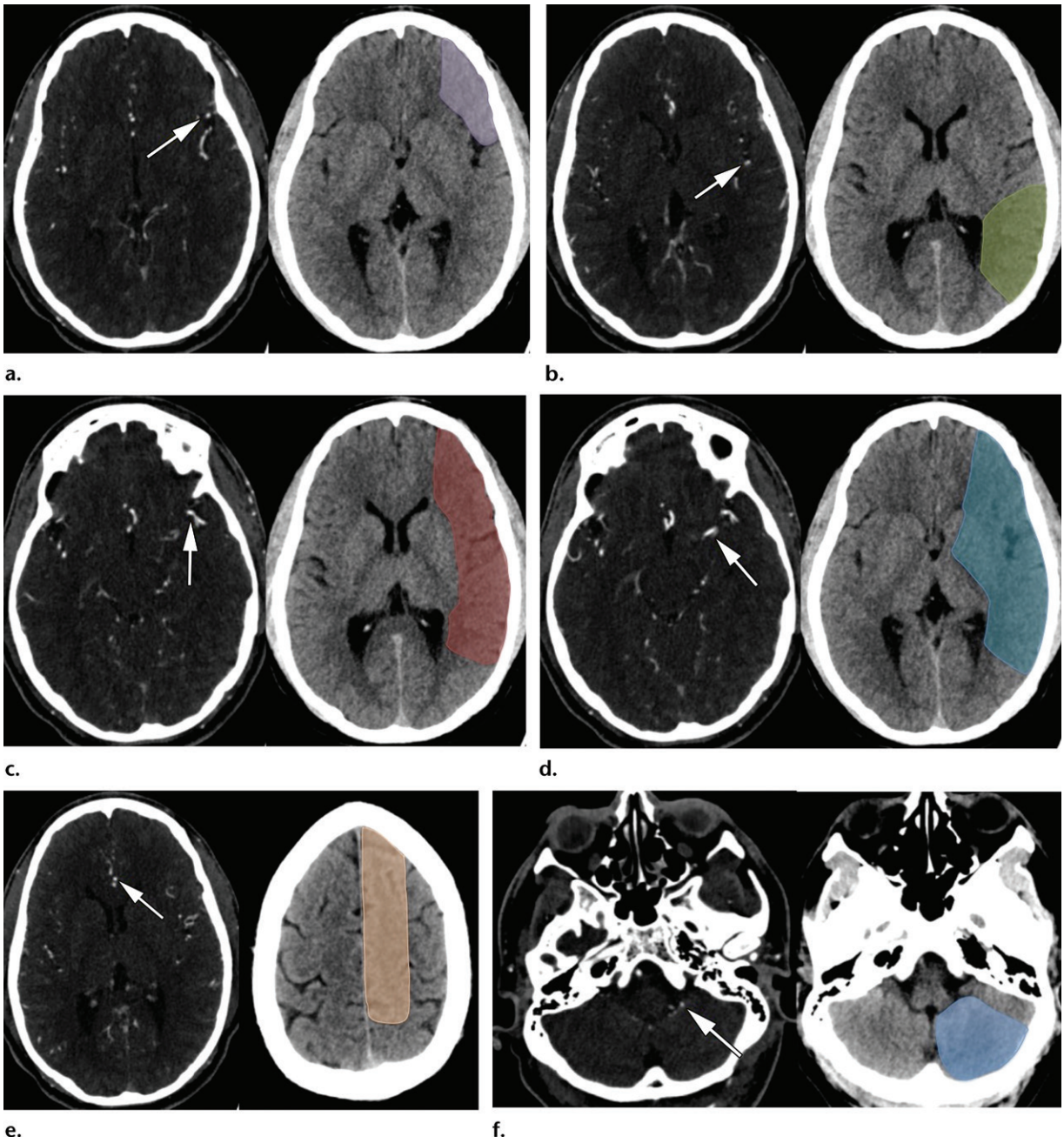

Figure 8. Common stroke syndromes. **(a)** Axial CT angiogram (left) shows the left superior M2 vessel (arrow). Along with the anterior temporal artery, the M2 segment perfuses the left frontal lobe and frontal operculum (purple region on nonenhanced CT image [right]). The frontal operculum contains the Broca area in the dominant hemisphere, and infarction may cause a nonfluent aphasia. **(b)** Axial CT angiogram (left) shows the left inferior M2 vessel (arrow), which typically perfuses the inferior parietal and temporal lobes (yellow region on nonenhanced CT image [right]). Infarction in this region in the dominant hemisphere could cause a fluent (Wernicke) aphasia. **(c)** Axial CT angiogram (left) shows the left MCA bifurcation (arrow). Occlusion can cause a pattern similar to occlusion of both M2 vessels but without significant involvement of the deep gray matter structures (red region on nonenhanced CT image [right]). **(d)** Axial CT angiogram (left) shows the proximal left M1 segment of the MCA (arrow). Occlusion in this segment typically causes hemiplegia and hemisensory loss owing to involvement of the cortex, basal ganglia, and internal capsule (blue region on nonenhanced CT image [right]). **(e)** Axial CT angiogram (left) shows the proximal left A2 segment of the ACA (arrow). The vascular territory of the ACA is parafalcine, and occlusion can cause contralateral lower extremity weakness and sensory loss (orange region on nonenhanced CT image [right]). **(f)** Axial CT angiogram (left) shows the left posterior inferior cerebellar artery (PICA) (arrow). The PICA often supplies the inferior medial cerebellum (blue region on nonenhanced CT image [right]), and infarction can cause a variety of symptoms, including ataxia.

may be clinically significant and can create falsely delayed arrival time values on perfusion CT images (48–50). However, management of proximal intracranial vascular stenoses is beyond the scope of this review. Thrombus density, distance to the terminal ICA, and length longer than 8 mm have been associated with worse functional outcome but are not used as criteria for EVT (51).

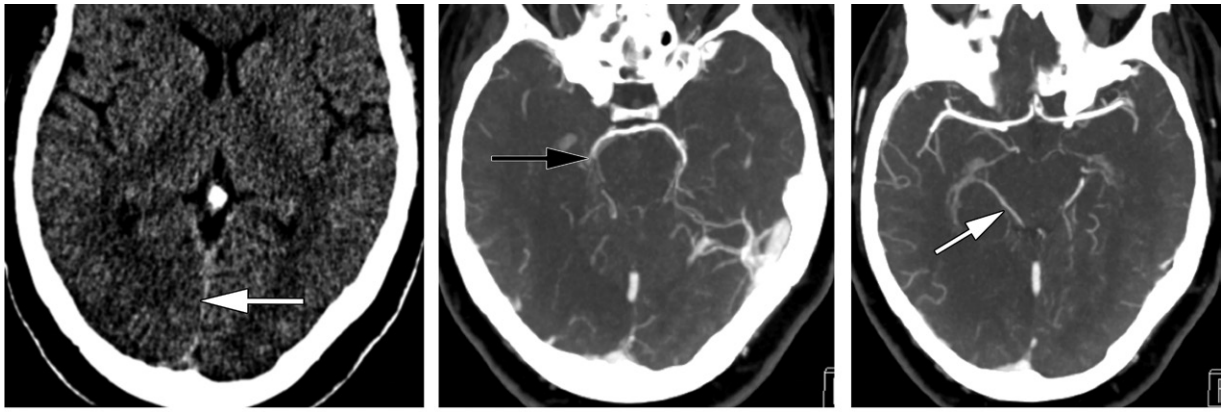

a. b. c.

Figure 9. Potential false-negative interpretation of a posterior cerebral artery (PCA) occlusion in a patient with new-onset vision changes. **(a)** Axial nonenhanced CT image shows mild hypoattenuation with loss of GWD in the medial right occipital lobe (arrow). **(b)** CT angiogram shows a patent proximal right PCA and a more distal and possibly contiguous enhanced vascular structure lateral to the midbrain and pons (arrow). **(c)** Axial thin-section source image from CT angiography shows that the distal structure is the basal vein of Rosenthal (arrow), a common confounder when assessing the patency of the PCA, which is occluded in this case.

It is important to evaluate initial CT angiograms of the neck at the scanner console to identify areas of critical stenosis, dissection, or vessel tortuosity. These findings can help inform the plan for EVT. CT angiograms can depict clinically relevant severe ICA stenosis at the cervical ICA origin (>70% narrowing), although heavy circumferential calcifications can lead to overestimation of the degree of narrowing.

Atherosclerotic disease of carotid origin and embolus associated with untreated atrial fibrillation are some of the most common causes of stroke in adults (52). Spontaneous arterial dissection is more common in patients younger than 40 years or after acute vascular trauma.

Multiplanar and MIP reconstructions aid in rapid screening of patency and vessel contour of the cervical carotid arteries as well as in demonstrating underlying vascular abnormalities, such as fibromuscular dysplasia. However, MIP images may poorly depict small intimal flaps in the carotid arteries, and evaluation of the vertebral arteries is complicated by the bony foramina. Evaluation of the cervical arteries in multiple planes is important, as pseudoaneurysms and dissections may be better visualized in the coronal and sagittal planes than on axial images.

At perfusion CT, it is important to identify extracranial narrowing that decreases the rate of intracranial flow. This can cause an abnormal appearance at perfusion CT and lead to misinterpretation of imaging findings, as discussed in the next section (48, 49).

Pitfalls of Image Review.—CT angiography can be challenging owing to the complexity of the anatomy, the number of images obtained, and patient cooperation. Images obtained before a stroke can be indispensable, particularly in confirmation of chronic vessel occlusions.

Late-phase CT angiography can lead to extensive venous attenuation that complicates interpretation by introducing distracting vessels and veins that can be confused with patent arteries. When venous contamination is present, it is essential to carefully trace the arteries, particularly the posterior cerebral arteries (PCAs) to avoid mistaking a patent basal vein of Rosenthal for a patent distal PCA segment (Fig 9).

Hypoattenuation on CT angiography source images has been studied as a correlate of low CBV in brain regions. CT angiography may be superior to nonenhanced CT alone for identification of parenchymal ischemic change (28). Studies have also shown that CT angiography source images and diffusion-weighted images are more accurate at depicting core infarct volume than nonenhanced CT images (28,53).

Like perfusion CT, CT angiography is flow and timing dependent and demonstrates tissue viability on the basis of hemodynamic parameters. For this reason, CT angiography source images have the potential to overestimate core infarct volume in regions of poor but not critical hypoperfusion. This overestimation can lead to inaccurate patient selection and underuse of EVT in patients who might benefit from treatment (28,54,55).

Collateral vessels can be viewed at single-phase, dual-phase, or multiphase CT angiography. Images must be acquired and reviewed by using at least arterial and delayed phases. The vessels can then be classified as good or poor by comparing the attenuation to that of the contralateral uninvolved hemisphere (33).

In regions of ischemia caused by long-segment proximal vascular occlusion, there may be a de-

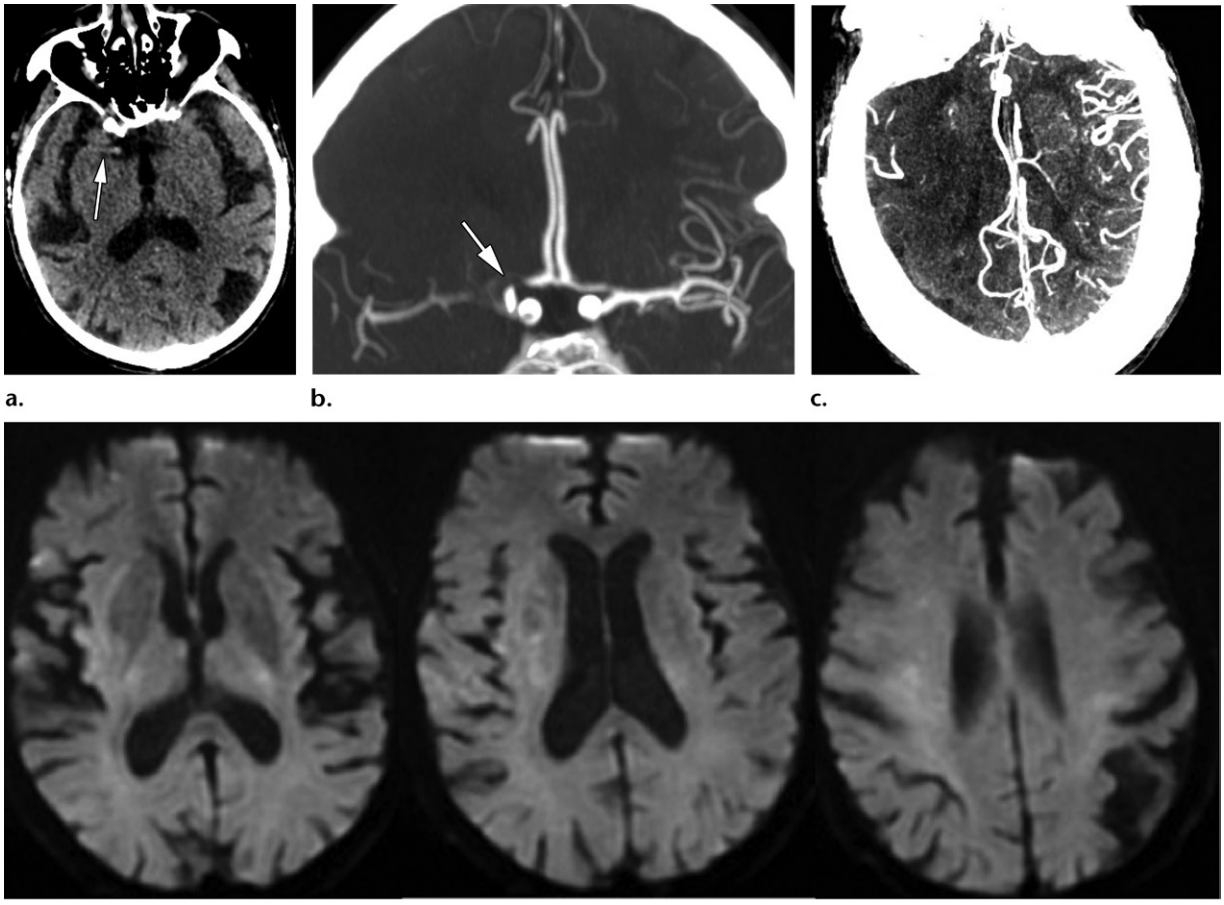

Figure 10. Poor collateral flow with early ischemia in a hospital visitor who collapsed after abrupt onset of left hemiparesis. **(a)** Nonenhanced CT image less than 30 minutes after stroke shows a hyperattenuating MCA sign (arrow) but is otherwise normal without subtle or well-established ischemic hypoattenuation, not surprising given the hyperacute manifestation. **(b)** Coronal thick-section MIP CT angiogram shows a T occlusion of the right ICA terminus involving the proximal M1 and A1 segments (arrow). **(c)** Axial thick-section MIP image of collateral vessels obtained in the arterial phase shows absent enhancement in over 50% of the territory at risk, suggestive of a malignant pattern with both vascular and parenchymal window and level settings. Given the hyperacute manifestation, normal nonenhanced CT findings, and immediate availability of the interventional team in a patient with a poor collateral pattern likely to progress to a large infarction, the decision was made to perform rapid EVT after thrombolysis with intravenous tPA. **(d)** Diffusion-weighted images obtained after removal of a right M1 thrombus show only trace final infarct in the right MCA territory.

layed arrival time of contrast material with relatively maintained collateral flow. In this context, reviewing arterial single-phase MIP images may be misleading.

For example, a region with intermediate collaterals distal to a long-segment occlusion might be labeled incorrectly as a poor or malignant pattern if the images are obtained too early in the arterial phase. This may inappropriately exclude some patients from receiving treatment with EVT (56,57) (Fig 10).

The ASPECTS system partially addresses this pitfall by using multiphase CT angiography. Collateral flow is categorized as good, intermediate, or poor on the basis of interhemispheric comparisons corrected for contrast material arrival time.

Other advantages of multiphase CT angiography include low cost of implementation and relative insensitivity to patient motion (33).

Perfusion CT

Technique

Dynamic or first-pass perfusion CT is performed by sequentially imaging a defined section of tissue after a single high-flow bolus of contrast material is administered. The same section is imaged multiple times in cine mode as the bolus passes to track the degree of attenuation at both the tissue and arterial levels as a function of time.

Older CT scanners with narrow detectors provided craniocaudal coverage of a limited section of the brain only. Modern scanners with helical capability and broader z-direction detectors can perform whole-brain perfusion CT.

As with CT angiography, an 18- or 20-gauge peripheral needle is preferred to achieve optimal contrast agent flow rates with a saline chaser of at least 15–20 mL. A minimum contrast material

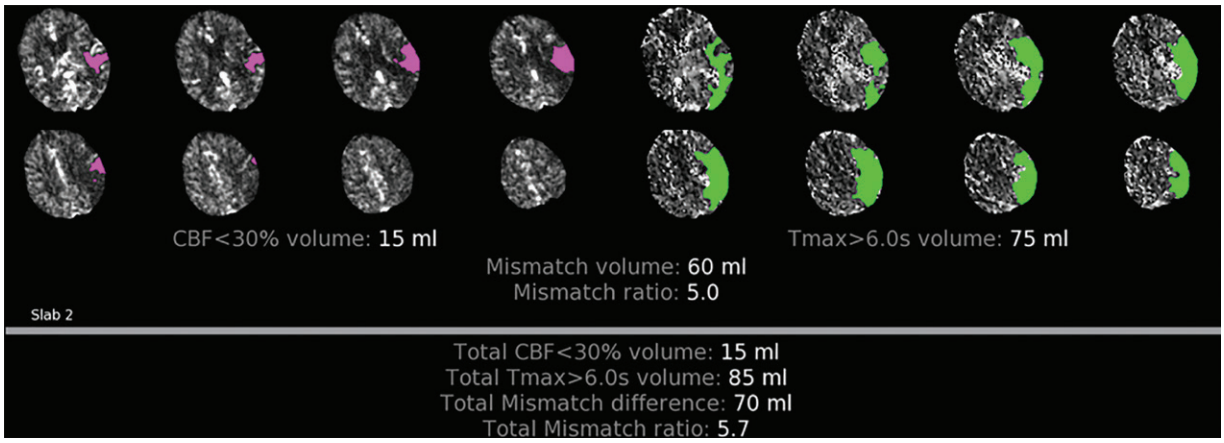

Figure 11. Perfusion CT findings favorable for EVT in an 85-year-old woman with atrial fibrillation who had received intravenous tPA for right MCA syndrome. CT angiography showed a right M1 occlusion extending to the inferior M2 division (not shown). CT perfusion images 10 hours after last known normal show a small 15-mL region of critical cerebral blood flow (CBF) reduction (CBF < 30% [purple]) surrounded by a larger 75-mL region of delayed transit time (time to maximum of the tissue residue function [T_{max}] > 6 seconds [green]) for a T_{max}-CBF mismatch ratio of 5. On the basis of these favorable perfusion CT findings, the patient was referred for EVT.

injection of 40 mL with a minimum rate of 4 mL/sec by using power injection is recommended. A higher rate of injection forms a tighter bolus and helps improve hemodynamic maps.

Technique should be optimized to the particular scanner, but 70–90 kVp and 100–200 mAs are recommended to keep the total radiation dose as low as reasonably achievable. In cine mode, one image per second should be acquired over a period of at least 50–60 seconds. Perfusion CT can be performed concurrently with or separately from CT angiography (58,60–62).

Automated or semiautomated postprocessing of the CT perfusion data generates multiple perfusion maps (38,58,59). Perfusion parameter calculations are performed using deconvolution approaches. The methodologies of different deconvolution algorithms are beyond the scope of this review (63).

Because attenuation change is linearly associated with the concentration of iodinated contrast material in a region, absolute values of perfusion parameters can be calculated. Cerebral blood flow (CBF) and time to maximum enhancement are among the most accurate values for use in acute stroke evaluation (64,65). Automated software platforms can generate qualitative and quantitative maps of ischemic lesion volumes from perfusion CT data with automatically selected arterial and venous inputs. The arterial inflow region of interest (ROI) is usually located in the A2 segment of the ACA or the M2 segment of the MCA. The venous ROI is selected over the dural venous confluence.

Even small differences in vessel ROI selection can result in substantial differences on the maps and in reported tissue values, so assessing the imaging input quality is important. To ensure high-quality perfusion CT images, it is also important to assess for patient motion, adequate attenuation of the contrast material bolus, and sufficiently long acquisition time to avoid truncation of the tissue and vessel time-attenuation curves (36,63).

Image Review

Tips and Pearls for Image Review.—Using the time-attenuation curves generated from initial ROI selection, color-coded perfusion parameter maps can be generated automatically or semiautomatically. Parameters demonstrated on these maps include CBF, time to maximum of the tissue residue function (T_{max}), CBV, and mean transit time. Only CBF and T_{max} have been widely studied in recent randomized clinical trials.

For example, in the CT arms of the DAWN and DEFUSE 3 trials, automated perfusion CT software estimated core infarct volume on the basis of a less than 30% threshold for CBF reduction and penumbral volume on the basis of a threshold greater than 6 seconds for prolongation of T_{max} (8,9). Mismatch ratios and ischemic volumes can be calculated, displayed, and used for clinical trial enrollment, depending on the specific eligibility criteria (Figs 11, 12).

The accuracy of perfusion CT for helping distinguish large (>100 mL) from small (<50–70 mL) core infarct volumes in EVT selection has been studied compared with a DWI reference standard (55,66–68). Use of perfusion CT has been increasing since its successful use in helping determine eligibility for enrollment in subsets of patients in the recent late-window DAWN and DEFUSE 3 trials (8,9).

Perfusion CT is grouped with MRI in the updated 2018 American Heart Association–

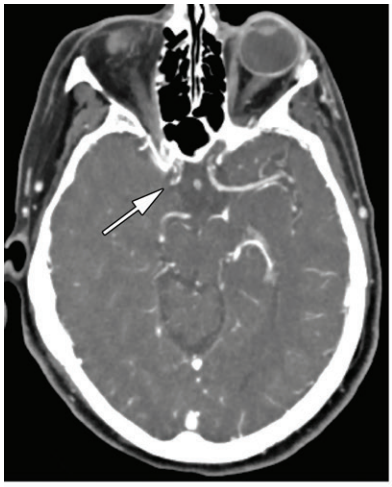

a.

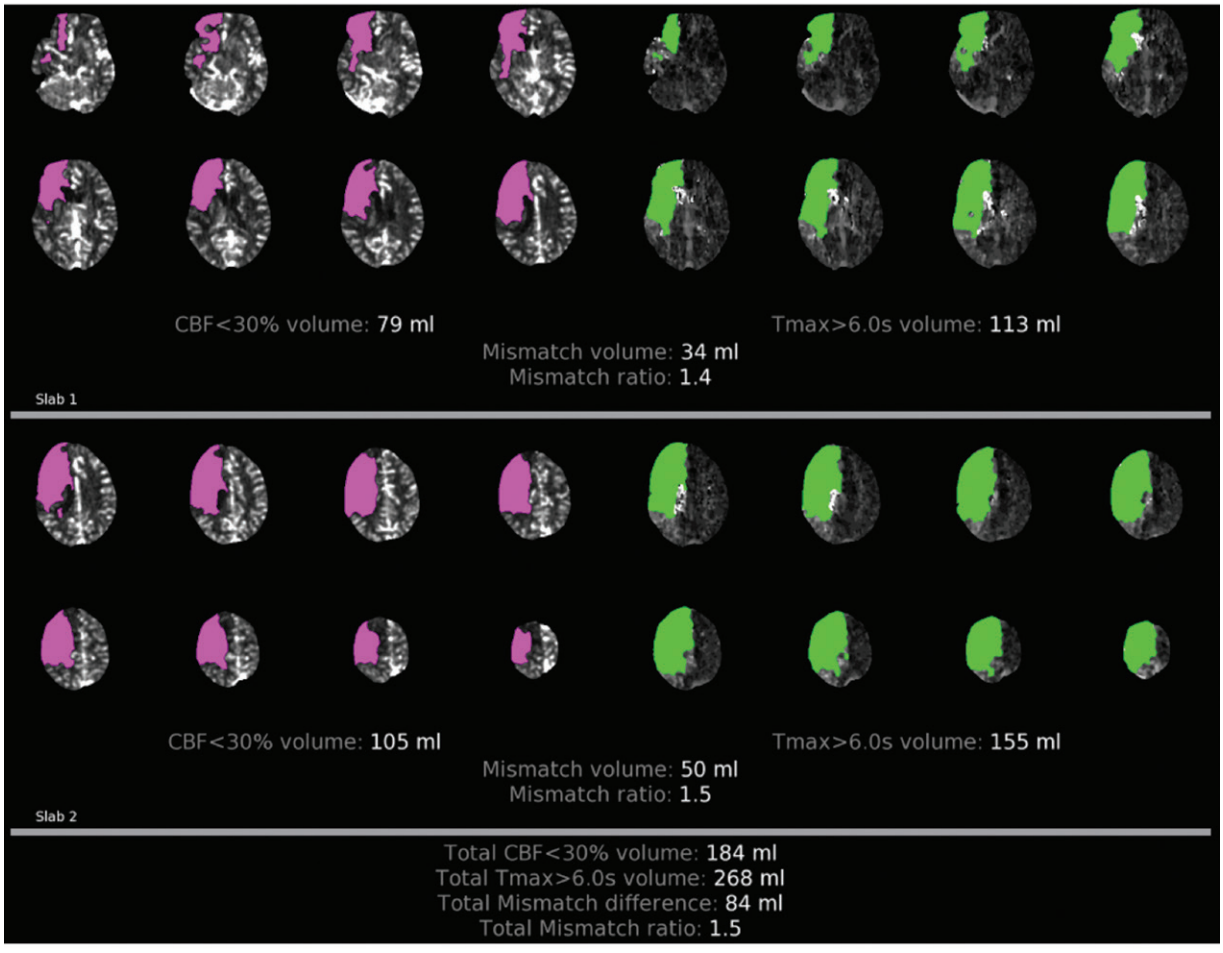

b.

Figure 12. Perfusion CT mismatch findings unfavorable for EVT in a 54-year-old woman with a history of coronary artery disease and hypertension who awoke with right hemispheric symptoms. **(a)** Axial CT angiogram shows complete occlusion of the right ICA and distal M1 and M2 (arrow). **(b)** Perfusion CT images show a large 105-mL region of critical cerebral blood flow (CBF) reduction (CBF < 30% [purple]) surrounded by a larger 155-mL region of delayed transit time (T_{max} > 6 sec [green]) for a T_{max}-CBF mismatch ratio of 1.5. The patient was not a candidate for intravenous tPA; on the basis of these unfavorable findings, EVT was not performed.

American Stroke Association guidelines for early management of patients with acute ischemic stroke, which states, "in selected patients with AIS [acute ischemic stroke] within 6 to 24 hours of last known normal who have LVO in the anterior circulation, obtaining CTP [CT perfusion imaging], DW-MRI [diffusion-weighted MRI], or MRI perfusion is recommended to aid in patient selection for mechanical thrombectomy, but only when imaging and other eligibility criteria from RCTs [randomized controlled trials] showing benefit are being strictly applied in selecting patients for mechanical thrombectomy" (3, p e59).

However, in the recent Hermes meta-analysis of early-window EVT trials and in a subgroup analysis of the DEFUSE 3 late-window trial that were presented at the 2018 American Heart Association International Stroke Conference,

DWI was found to be more efficient than perfusion CT when used to help select candidates for EVT. DWI was found to have higher odds ratios for selecting patients more likely to experience clinical improvement and functional independence (69).

Given this, it is not surprising that there is currently little consensus on the optimal imaging strategy for late-window EVT selection. Use of DWI, CT angiography of collateral vessels, and perfusion CT for core infarct volume assessment varies widely between different comprehensive stroke centers and in different clinical situations (8,9,66,70).

Additionally, recent trials have suggested that advanced CT and MRI can be used to extend the time window for intravenous tPA administration (71,72). The recent EXTEND (Extending the Time for Thrombolysis in Emergency Neurological Deficits) trial results have shown that patients benefit from treatment with intravenous tPA at 9 hours or after a wake-up stroke when they are selected using perfusion CT or perfusion MRI (73).

Tenecteplase is a newer intravenous tPA that is currently being investigated in late-window clinical trials. When perfusion CT is used for treatment selection, tenecteplase may provide stronger benefits up to 6 hours after symptom onset (74).

Pitfalls of Image Review.—Potential pitfalls of perfusion CT include motion artifact, poor signal-to-noise ratio from a suboptimal contrast material bolus, faulty arterial and venous input functions, and truncation of the tissue and vascular time-attenuation flow curves from a shortened acquisition time.

It is important to identify the degree of motion to decide whether the images are of adequate quality. Moderate-to-severe motion artifact occurs frequently, and one study reported that it occurred in 25% of patients (75).

Although automated perfusion software generates volumetric data for core and penumbra, it is important to be aware of its potential technical and clinical pitfalls. The time-attenuation curves should be evaluated to ensure appropriate location of the ROI in a vessel that runs nearly perpendicular to the imaging plane to avoid volume averaging with the vessel wall and surrounding structures. Slow flow in a stenotic major vessel selected for the arterial input function (eg, chronic carotid occlusion) will result in inaccurate relative parameter values.

The effect of truncated time-attenuation curves has also been a concern (68,69,79). Perfusion CT protocols less than 60 seconds in length can overestimate infarct core volume, since perfusion parameter values may be underestimated in voxels with incomplete bolus tracking (77-79).

Poor signal-to-noise ratio can result when insufficient contrast material reaches the imaging voxel. This can be caused by factors such as poor cardiac output associated with atrial fibrillation (commonly associated with acute embolic stroke) or unsuspected venous or arterial stenoses delaying the arrival of contrast material at the circle of Willis (48,63,49).

Moreover, thresholds for determining core and penumbra can vary between vendors and between postprocessing platforms (68,69). Thresholds for determining irreversible ischemia likely vary with time after stroke, quality of collateral flow, and ischemic preconditioning (11,55). Perfusion CT thresholds can also be unreliable in the presence of old infarcts, partial reperfusion, or hyperemia associated with compensatory vasodilatation.

Stroke Mimics

Potential acute stroke mimics include intracranial masses due to primary or metastatic malignancy, cerebritis, cerebral abscess, and posterior reversible encephalopathy syndrome (PRES). Most of these pathologic processes cause vasogenic edema and accentuation of—rather than loss of—GWD. Low-grade gliomas and other hypoattenuating lesions without surrounding vasogenic edema may require use of MRI for definitive diagnosis (Fig 13).

Increased gyriform enhancement with mass effect in subacute infarction may be indistinguishable from high-grade glioma. Metastases, cerebritis, abscess, demyelinating disease, and PRES can all mimic subacute infarction by blurring or effacing GWD owing to mass effect and displacement (Fig 13).

Contrast material staining after EVT can mimic acute hemorrhage. Dual-energy CT iodine maps and virtual nonenhanced CT images can help confirm that intracranial hyperattenuation is due to iodine leakage through a nonintact blood-brain barrier (16,79).

Perfusion CT can also be useful in stroke differential diagnosis by helping distinguish wedge-shaped perfusion deficits caused by arterial occlusive emboli from other flow derangements, such as those caused by seizure, hypoglycemia, or hyperglycemia (49).

Conclusion

CT evaluation of acute ischemic stroke is robust, rapid, and widely available. The DAWN and DEFUSE 3 trials proved that EVT results in improved outcomes and functional independence

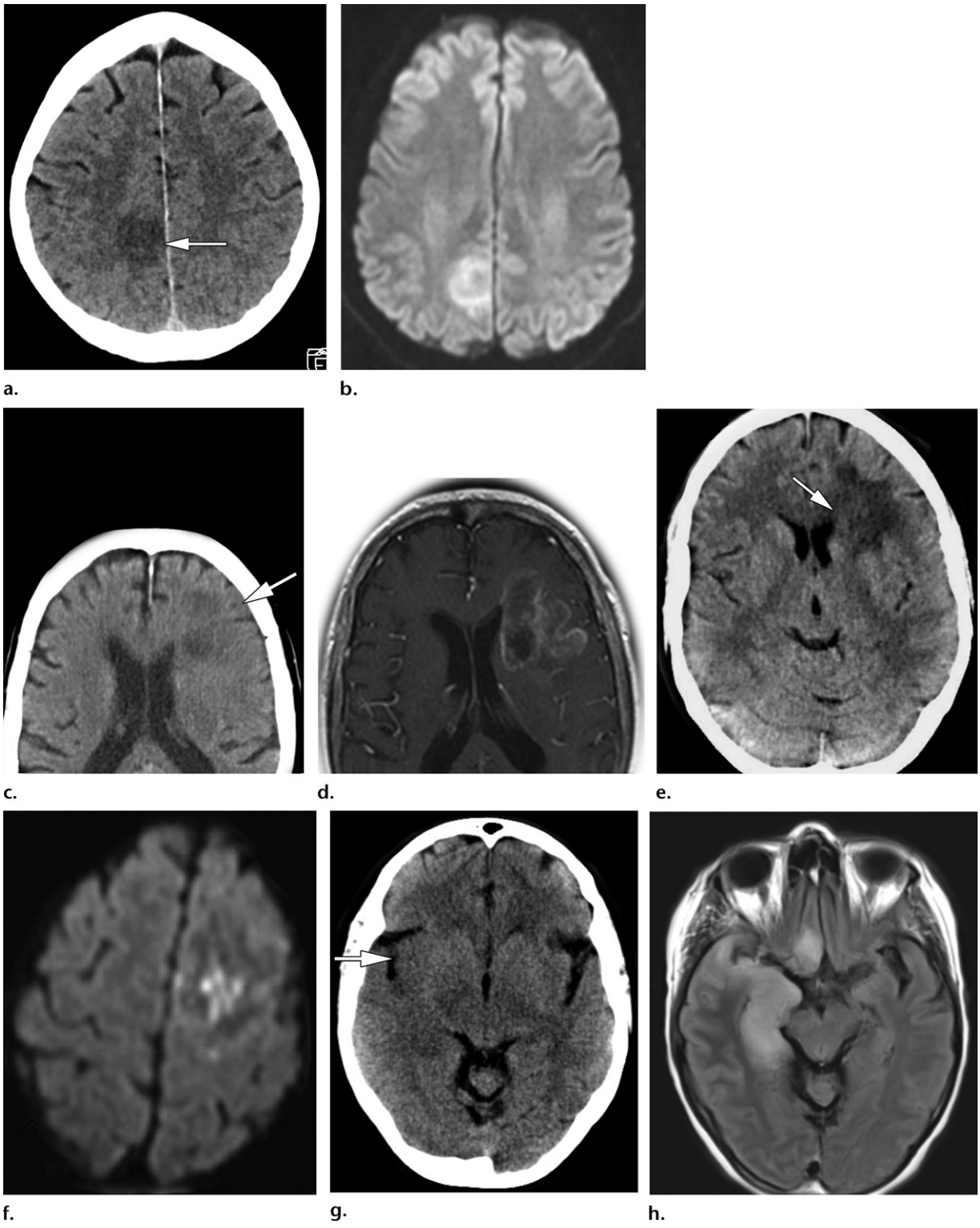

Figure 13. Stroke mimics caused by nonspecific hypoattenuating lesions at nonenhanced CT. **(a)** Nonenhanced CT image in a 58-year-old man with confusion shows cortical effacement from a well-circumscribed rounded area of hypoattenuation with loss of GWD in the medial right parietal lobe (arrow). **(b)** Subsequent FLAIR (fluid-attenuated inversion-recovery) image shows that the lesion is hyperintense. DWI showed no diffusion restriction in the lesion, which was confirmed at biopsy to be a low-grade glioma. **(c)** Admission nonenhanced CT image in another patient shows an irregular lesion with patchy hypoattenuation (arrow). **(d)** Contrast-enhanced T1-weighted MR image shows serpentine irregular surrounding enhancement. These findings are suggestive of a subacute evolving infarct, but the lesion was proved to represent a left frontal glioblastoma multiforme. **(e)** Nonenhanced CT image in another patient shows subcortical and gray-white matter junction left frontal lobe hypoattenuation (arrow), which is suggestive of vasogenic edema but nonspecific. **(f)** Diffusion-weighted image shows diffusion restriction. Along with peripheral enhancement on postcontrast T1-weighted images (not shown), these findings helped confirm the final diagnosis of cerebral abscess. **(g)** Nonenhanced CT image in a young patient shows loss of GWD in the right insula and external capsule (arrow). **(h)** FLAIR image shows additional involvement of the right mesial temporal lobe, amygdala, and hypothalamic regions. The final diagnosis was herpes encephalitis.

even up to 24 hours after a stroke. Because of this, nonenhanced CT and CT angiography have become the community standards for selecting patients for intravenous tPA and EVT in both early and late time windows.

Although DWI is the reference standard for determining core infarct lesion volume, CT angiography and perfusion CT may be used when DWI is not available. These uses of CT may help distinguish patients with large infarct cores—who are least likely to benefit from and most likely to be harmed by EVT—from patients with small infarct cores.

Awareness of common findings, pearls, and pitfalls of multimodal stroke CT evaluation and interpretation has therefore become essential for providers caring for patients with acute stroke.

***Disclosures of Conflicts of Interest.*—A.S.V.** *Activities related to the present article:* disclosed no relevant relationships. *Activities not related to the present article:* institution received grants from Cerenovus, ENDOLOW trial, GE Healthcare, Imaging Core Lab, and Johnson & Johnson. *Other activities:* disclosed no relevant relationships. **M.G.** *Activities related to the present article:* disclosed no relevant relationships. *Activities not related to the present article:* author received payment from Medtronic, Mentice, Microvention, and Stryker for consulting; institution received grants from Medtronic and Stryker; author received payment from GE Healthcare for a licensing agreement. *Other activities:* disclosed no relevant relationships. **M.H.L.** *Activities related to the present article:* disclosed no relevant relationships. *Activities not related to the present article:* received grant from GE Healthcare; consultant to Takeda Pharmaceuticals and GE Healthcare; institution received research funding from GE Healthcare; institution received research software license from Siemens Healthineers. *Other activities:* patents pending for portable electrical impedance spectroscopy device, artificial intelligence for use in CT of brain hemorrhage, and artifical intelligence to depict collaterals.

References

1. Tomandl BF, Klotz E, Handschu R, et al. Comprehensive imaging of ischemic stroke with multisection CT. RadioGraphics 2003;23(3):565–592.
2. National Institute of Neurological Disorders and Stroke rt-PA Stroke Study Group. Tissue plasminogen activator for acute ischemic stroke. N Engl J Med 1995;333(24):1581–1587.
3. Powers WJ, Rabinstein AA, Ackerson T, et al. 2018 Guidelines for the Early Management of Patients With Acute Ischemic Stroke: A Guideline for Healthcare Professionals From the American Heart Association/American Stroke Association. Stroke 2018;49(3):e46–e110. [Published corrections appear in Stroke 2018;49(3):e138 and Stroke 2018;49(6):e233–e234.] https://doi.org/10.1161/STR.0000000000000158.
4. Tomura N, Uemura K, Inugami A, Fujita H, Higano S, Shishido F. Early CT finding in cerebral infarction: obscuration of the lentiform nucleus. Radiology 1988; 168(2):463–467.
5. Truwit CL, Barkovich AJ, Gean-Marton A, Hibri N, Norman D. Loss of the insular ribbon: another early CT sign of acute middle cerebral artery infarction. Radiology 1990;176(3):801–806.
6. Dippel DW, Du Ry van Beest Holle M, van Kooten F, Koudstaal PJ. The validity and reliability of signs of early infarction on CT in acute ischaemic stroke. Neuroradiology 2000;42(9):629–633.
7. Wardlaw JM, Mielke O. Early signs of brain infarction at CT: observer reliability and outcome after thrombolytic treatment—systematic review. Radiology 2005;235(2):444–453.
8. Nogueira RG, Jadhav AP, Haussen DC, et al. Thrombectomy 6 to 24 Hours after Stroke with a Mismatch between Deficit and Infarct. N Engl J Med 2018;378(1):11–21.
9. Albers GW, Marks MP, Kemp S, et al. Thrombectomy for Stroke at 6 to 16 Hours with Selection by Perfusion Imaging. N Engl J Med 2018;378(8):708–718.
10. Sims JR, Gharai LR, Schaefer PW, et al. ABC/2 for rapid clinical estimate of infarct, perfusion, and mismatch volumes. Neurology 2009;72(24):2104–2110.
11. Schellinger PD, Bryan RN, Caplan LR, et al. Evidence-based guideline: the role of diffusion and perfusion MRI for the diagnosis of acute ischemic stroke: report of the Therapeutics and Technology Assessment Subcommittee of the American Academy of Neurology. Neurology 2010;75(2):177–185. [Published correction appears in Neurology 2010;75(10):938.] https://doi.org/10.1212/WNL.0b013e3181e7c9dd.
12. González RG. Imaging-guided acute ischemic stroke therapy: from "time is brain" to "physiology is brain." AJNR Am J Neuroradiol 2006;27(4):728–735.
13. Kanekar SG, Zacharia T, Roller R. Imaging of stroke. II. Pathophysiology at the molecular and cellular levels and corresponding imaging changes. AJR Am J Roentgenol 2012;198(1):63–74.
14. Kelly AG, Hellkamp AS, Olson D, Smith EE, Schwamm LH. Predictors of rapid brain imaging in acute stroke: analysis of the Get with the Guidelines—Stroke program. Stroke 2012;43(5):1279–1284.
15. ACR-ASNR-SPR Practice Parameter for the Performance of Computed Tomography (CT) of the Brain. https://www.acr.org/-/media/ACR/Files/Practice-Parameters/CT-Brain.pdf. Revised 2015. Accessed April 2, 2019.
16. Potter CA, Sodickson AD. Dual-Energy CT in Emergency Neuroimaging: added Value and Novel Applications. RadioGraphics 2016;36(7):2186–2198.
17. Pomerantz SR, Kamalian S, Zhang D, et al. Virtual monochromatic reconstruction of dual-energy unenhanced head CT at 65-75 keV maximizes image quality compared with conventional polychromatic CT. Radiology 2013;266(1):318–325.
18. Perry JJ, Stiell IG, Sivilotti ML, et al. Sensitivity of computed tomography performed within six hours of onset of headache for diagnosis of subarachnoid haemorrhage: prospective cohort study. BMJ 2011;343:d4277.
19. Lee H, Yune S, Mansouri M, et al. An explainable deep-learning algorithm for the detection of acute intracranial haemorrhage from small datasets. Nat Biomed Eng 2019;3(3):173–182.
20. Kamalian S, Kemmling A, Borgie RC, et al. Admission insular infarction >25% is the strongest predictor of large mismatch loss in proximal middle cerebral artery stroke. Stroke 2013;44(11):3084–3089.
21. Kucinski T. Unenhanced CT and acute stroke physiology. Neuroimaging Clin N Am 2005;15(2):397–407, xi–xii.
22. Pexman JH, Barber PA, Hill MD, et al. Use of the Alberta Stroke Program Early CT Score (ASPECTS) for assessing CT scans in patients with acute stroke. AJNR Am J Neuroradiol 2001;22(8):1534–1542.
23. Kuang H, Najm M, Chakraborty D, et al. Automated ASPECTS on Noncontrast CT Scans in Patients with Acute Ischemic Stroke Using Machine Learning. AJNR Am J Neuroradiol 2019;40(1):33–38.
24. Leys D, Pruvo JP, Godefroy O, Rondepierre P, Leclerc X. Prevalence and significance of hyperdense middle cerebral artery in acute stroke. Stroke 1992;23(3):317–324.
25. Mair G, Boyd EV, Chappell FM, et al. Sensitivity and specificity of the hyperdense artery sign for arterial obstruction in acute ischemic stroke. Stroke 2015;46(1):102–107.
26. Barber PA, Demchuk AM, Hudon ME, Pexman JH, Hill MD, Buchan AM. Hyperdense sylvian fissure MCA "dot" sign: a CT marker of acute ischemia. Stroke 2001;32(1):84–88.
27. Lev MH, Farkas J, Gemmete JJ, et al. Acute stroke: improved nonenhanced CT detection—benefits of soft-copy interpretation by using variable window width and center level settings. Radiology 1999;213(1):150–155.
28. Camargo EC, Furie KL, Singhal AB, et al. Acute brain infarct: detection and delineation with CT angiographic

source images versus nonenhanced CT scans. Radiology 2007;244(2):541–548.
29. Goldmakher GV, Camargo EC, Furie KL, et al. Hyperdense basilar artery sign on unenhanced CT predicts thrombus and outcome in acute posterior circulation stroke. Stroke 2009;40(1):134–139.
30. Riedel CH, Jensen U, Rohr A, et al. Assessment of thrombus in acute middle cerebral artery occlusion using thin-slice nonenhanced computed tomography reconstructions. Stroke 2010;41(8):1659–1664.
31. Dittrich R, Akdeniz S, Kloska SP, et al. Low rate of contrast-induced nephropathy after CT perfusion and CT angiography in acute stroke patients. J Neurol 2007;254(11):1491–1497.
32. ACR-ASNR-SPR Practice Parameter for the Performance and Interpretation of Cervicocerebral Computed Tomography Angiography (CTA) of the Brain. https://www.acr.org/-/media/ACR/Files/Practice-Parameters/CervicoCerebralCTA.pdf. Revised 2015. Accessed April 2, 2019.
33. Menon BK, d'Esterre CD, Qazi EM, et al. Multiphase CT Angiography: a New Tool for the Imaging Triage of Patients with Acute Ischemic Stroke. Radiology 2015;275(2):510–520.
34. Kortman HG, Smit EJ, Oei MT, Manniesing R, Prokop M, Meijer FJ. 4D-CTA in neurovascular disease: a review. AJNR Am J Neuroradiol 2015;36(6):1026–1033.
35. Deng K, Liu C, Ma R, et al. Clinical evaluation of dual-energy bone removal in CT angiography of the head and neck: comparison with conventional bone-subtraction CT angiography. Clin Radiol 2009;64(5):534–541.
36. Buerke B, Puesken M, Wittkamp G, et al. Bone subtraction CTA for transcranial arteries: intra-individual comparison with standard CTA without bone subtraction and TOF-MRA. Clin Radiol 2010;65(6):440–446.
37. McCollough CH, Leng S, Yu L, Fletcher JG. Dual- and Multi-Energy CT: principles, Technical Approaches, and Clinical Applications. Radiology 2015;276(3):637–653.
38. de Lucas EM, Sánchez E, Gutiérrez A, et al. CT protocol for acute stroke: tips and tricks for general radiologists. RadioGraphics 2008;28(6):1673–1687.
39. Yeo LL, Paliwal P, Teoh HL, et al. Assessment of intracranial collaterals on CT angiography in anterior circulation acute ischemic stroke. AJNR Am J Neuroradiol 2015;36(2):289–294.
40. Maas MB, Lev MH, Ay H, et al. Collateral vessels on CT angiography predict outcome in acute ischemic stroke. Stroke 2009;40(9):3001–3005.
41. Miteff F, Levi CR, Bateman GA, Spratt N, McElduff P, Parsons MW. The independent predictive utility of computed tomography angiographic collateral status in acute ischaemic stroke. Brain 2009;132(Pt 8):2231–2238.
42. Souza LC, Yoo AJ, Chaudhry ZA, et al. Malignant CTA collateral profile is highly specific for large admission DWI infarct core and poor outcome in acute stroke. AJNR Am J Neuroradiol 2012;33(7):1331–1336.
43. Goyal M, Menon BK, Almekhlafi MA, Demchuk A, Hill MD. The Need for Better Data on Patients with Acute Stroke Who Are Not Treated Because of Unfavorable Imaging. AJNR Am J Neuroradiol 2017;38(3):424–425.
44. Rocha M, Jovin TG. Fast Versus Slow Progressors of Infarct Growth in Large Vessel Occlusion Stroke: Clinical and Research Implications. Stroke 2017;48(9):2621–2627.
45. ASPECTS Collateral Score. http://www.aspectsinstroke.com/collateral-scoring/. Accessed April 2, 2019.
46. Sun CH, Connelly K, Nogueira RG, et al. ASPECTS decay during inter-facility transfer predicts patient outcomes in endovascular reperfusion for ischemic stroke: a unique assessment of dynamic physiologic change over time. J Neurointerv Surg 2015;7(1):22–26.
47. Aminoff MJ, Josephson SA, eds. Aminoff's Neurology and General Medicine. 5th ed. London, England: Academic Press/Elsevier, 2014.
48. Allmendinger AM, Tang ER, Lui YW, Spektor V. Imaging of stroke. I. Perfusion CT: overview of imaging technique, interpretation pearls, and common pitfalls. AJR Am J Roentgenol 2012;198(1):52–62.
49. Lui YW, Tang ER, Allmendinger AM, Spektor V. Evaluation of CT perfusion in the setting of cerebral ischemia: patterns and pitfalls. AJNR Am J Neuroradiol 2010;31(9):1552–1563.
50. Holmstedt CA, Turan TN, Chimowitz MI. Atherosclerotic intracranial arterial stenosis: risk factors, diagnosis, and treatment. Lancet Neurol 2013;12(11):1106–1114.
51. Borst J, Berkhemer OA, Santos EMM, et al. Value of Thrombus CT Characteristics in Patients with Acute Ischemic Stroke. AJNR Am J Neuroradiol 2017;38(9):1758–1764.
52. Benjamin EJ, Virani SS, Callaway CW, et al. Heart Disease and Stroke Statistics—2018 Update: A Report From the American Heart Association. Circulation 2018;137(12):e67–e492. [Published correction appears in Circulation 2018;137(12):e493.] https://doi.org/10.1161/CIR.0000000000000558.
53. Schramm P, Schellinger PD, Fiebach JB, et al. Comparison of CT and CT angiography source images with diffusion-weighted imaging in patients with acute stroke within 6 hours after onset. Stroke 2002;33(10):2426–2432.
54. Pulli B, Schaefer PW, Hakimelahi R, et al. Acute ischemic stroke: infarct core estimation on CT angiography source images depends on CT angiography protocol. Radiology 2012;262(2):593–604.
55. Schaefer PW, Souza L, Kamalian S, et al. Limited reliability of computed tomographic perfusion acute infarct volume measurements compared with diffusion-weighted imaging in anterior circulation stroke. Stroke 2015;46(2):419–424.
56. Christoforidis GA, Mohammad Y, Kehagias D, Avutu B, Slivka AP. Angiographic assessment of pial collaterals as a prognostic indicator following intra-arterial thrombolysis for acute ischemic stroke. AJNR Am J Neuroradiol 2005;26(7):1789–1797.
57. Reid M, Famuyide AO, Forkert ND, et al. Accuracy and Reliability of Multiphase CTA Perfusion for Identifying Ischemic Core. Clin Neuroradiol 2018 Aug 21. [Epub ahead of print] [Published correction appears in Clin Neuroradiol 2019 Jun 3.] https://doi.org/10.1007/s00062-018-0717-x.
58. Hoeffner EG, Case I, Jain R, et al. Cerebral perfusion CT: technique and clinical applications. Radiology 2004;231(3):632–644.
59. Srinivasan A, Goyal M, Al Azri F, Lum C. State-of-the-art imaging of acute stroke. RadioGraphics 2006;26(suppl 1):S75–S95.
60. Eastwood JD, Lev MH, Provenzale JM. Perfusion CT with iodinated contrast material. AJR Am J Roentgenol 2003;180(1):3–12.
61. Christensen S, Lansberg MG. CT perfusion in acute stroke: practical guidance for implementation in clinical practice. J Cereb Blood Flow Metab 2018 Oct 22:271678X18805590 [Epub ahead of print].
62. ACR-ASNR-SPR Practice Parameter for the Performance of Computed Tomography (CT) Perfusion in Neuroradiologic Imaging. https://www.acr.org/-/media/ACR/Files/Practice-Parameters/ct-perfusion.pdf. Revised 2017. Accessed April 2, 2019.
63. Konstas AA, Goldmakher GV, Lee TY, Lev MH. Theoretic basis and technical implementations of CT perfusion in acute ischemic stroke. II. Technical implementations. AJNR Am J Neuroradiol 2009;30(5):885–892.
64. Bivard A, Levi C, Spratt N, Parsons M. Perfusion CT in acute stroke: a comprehensive analysis of infarct and penumbra. Radiology 2013;267(2):543–550.
65. Campbell BC, Mitchell PJ, Kleinig TJ, et al. Endovascular therapy for ischemic stroke with perfusion-imaging selection. N Engl J Med 2015;372(11):1009–1018.
66. Goyal M, Menon BK, Derdeyn CP. Perfusion imaging in acute ischemic stroke: let us improve the science before changing clinical practice. Radiology 2013;266(1):16–21.
67. Kamalian S, Kamalian S, Maas MB, et al. CT cerebral blood flow maps optimally correlate with admission diffusion-weighted imaging in acute stroke but thresholds vary by postprocessing platform. Stroke 2011;42(7):1923–1928.
68. Kamalian S, Kamalian S, Konstas AA, et al. CT perfusion mean transit time maps optimally distinguish benign oligemia from true "at-risk" ischemic penumbra, but thresholds vary by postprocessing technique. AJNR Am J Neuroradiol 2012;33(3):545–549.

69. Campbell BCV, Majoie CBLM, Albers GW, et al. Penumbral imaging and functional outcome in patients with anterior circulation ischaemic stroke treated with endovascular thrombectomy versus medical therapy: a meta-analysis of individual patient-level data. Lancet Neurol 2019;18(1):46–55.
70. Leslie-Mazwi TM, Hirsch JA, Falcone GJ, et al. Endovascular Stroke Treatment Outcomes After Patient Selection Based on Magnetic Resonance Imaging and Clinical Criteria. JAMA Neurol 2016;73(1):43–49.
71. Thomalla G, Simonsen CZ, Boutitie F, et al. MRI-Guided Thrombolysis for Stroke with Unknown Time of Onset. N Engl J Med 2018;379(7):611–622.
72. Ma H, Campbell BCV, Parsons MW, et al. Thrombolysis Guided by Perfusion Imaging up to 9 Hours after Onset of Stroke. N Engl J Med 2019;380(19):1795–1803.
73. Schwamm LH, Wu O, Song SS, et al. Intravenous thrombolysis in unwitnessed stroke onset: MR WITNESS trial results. Ann Neurol 2018;83(5):980–993.
74. Parsons M, Spratt N, Bivard A, et al. A randomized trial of tenecteplase versus alteplase for acute ischemic stroke. N Engl J Med 2012;366(12):1099–1107.
75. Fahmi F, Beenen LF, Streekstra GJ, et al. Head movement during CT brain perfusion acquisition of patients with suspected acute ischemic stroke. Eur J Radiol 2013;82(12):2334–2341.
76. Borst J, Marquering HA, Beenen LF, et al. Effect of extended CT perfusion acquisition time on ischemic core and penumbra volume estimation in patients with acute ischemic stroke due to a large vessel occlusion. PLoS One 2015;10(3):e0119409.
77. Copen WA, Deipolyi AR, Schaefer PW, Schwamm LH, González RG, Wu O. Exposing hidden truncation-related errors in acute stroke perfusion imaging. AJNR Am J Neuroradiol 2015;36(4):638–645.
78. Schaefer PW, Mui K, Kamalian S, Nogueira RG, Gonzalez RG, Lev MH. Avoiding "pseudo-reversibility" of CT-CBV infarct core lesions in acute stroke patients after thrombolytic therapy: the need for algorithmically "delay-corrected" CT perfusion map postprocessing software. Stroke 2009;40(8):2875–2878.
79. Phan CM, Yoo AJ, Hirsch JA, Nogueira RG, Gupta R. Differentiation of hemorrhage from iodinated contrast in different intracranial compartments using dual-energy head CT. AJNR Am J Neuroradiol 2012;33(6):1088–1094.